Cover Page

Alpha Foundation for the Improvement of Mine Safety and Health

Final Technical Report

Project Title:	A Strong and Ductile High-Performance Pumpable Roof Support
Grant Number:	AFCTG22r2-161
Organization:	The University of Arizona
Principal Investigator:	Lianyang Zhang, Ph.D., P.E., F.ASCE
Graduate Students:	Sahand Motameni, Ph.D.; Saleh Ali, Khawaja, MS
Contact Information:	Email: lyzhang@arizona.edu Phone: 520-626-0532
Period of Performance:	January 1, 2023 – October 30, 2026

Acknowledgement/Disclaimer: This study was sponsored by the Alpha Foundation for the Improvement of Mine Safety and Health, Inc. (ALPHA FOUNDATION). The views, opinions and recommendations expressed herein are solely those of the authors and do not imply any endorsement by the ALPHA FOUNDATION, its Directors and staff.

Table of Contents

Cover Page 1

Table of Contents 2

1.0 Executive Summary 3

2.0 Problem Statement and Objective 4

2.1 Problem Statement 4

2.2 Objective 4

3.0 Research Approach 6

3.1 Identification of extremely light, highly compressible, micro-sized beads/spheres 6

3.2 Laboratory experiments using extremely light, highly compressible, micro-sized beads/spheres 7

3.3 Laboratory experiments using foam as top portion of specimens 7

3.4 Laboratory experiments on bagged specimens containing internal reinforcements 7

4.0 Research Findings and Accomplishments 9

4.1 Research findings 9

4.1.1 Identification of extremely light, highly compressible, micro-sized beads/spheres 9

4.1.2 Laboratory experiments using extremely light, highly compressible, micro-sized beads/spheres 9

4.1.3 Laboratory experiments using foam as top portion of specimens 10

4.1.4 Laboratory experiments on bagged specimens containing internal reinforcements 10

4.2 Accomplishments 11

5.0 Publication Record and Dissemination Efforts 12

6.0 Conclusions and Impact Assessment 13

7.0 Recommendations for Future Work 14

8.0 Appendices 15

App. 1: Identification of extremely light, highly compressible, micro-sized beads/spheres 15

App. 2: Laboratory experiments using extremely light, highly compressible, micro-sized beads/spheres 18

App. 3: Laboratory experiments using foam as top portion of specimens 35

App. 4: Laboratory experiments on bagged specimens containing internal reinforcements 42

9.0 Acknowledgement/Disclaimer 55

1.0 Progress Summary

The overall goal of this project is to further enhance the performance of pumpable roof supports (PRSs) by increasing their ductility while maintaining their peak and residual bearing capacities. To achieve this goal, the research has focused on the following major tasks:

- *Identification of Extremely Light, Highly Compressible, Micro-Sized Beads/Spheres*
  An extensive search was conducted to identify extremely light, highly compressible, micron-sized beads/spheres that can be incorporated into cementitious materials to form PRSs consisting of a highly deformable and ductile upper portion and a strong lower portion.
- *Laboratory Experiments Using Extremely Light, Highly Compressible, Micro-Sized Beads/Spheres as Additives*
  Using two types of extremely light, highly compressible, micron-sized beads/spheres as additives, both unbagged and bagged cylindrical specimens were prepared to study the effects of incorporated beads/spheres on the mechanical behavior (peak strength, strain at peak strength, and residual strength) of the cementitious material itself (unbagged specimens) and the pumpable support system (bagged specimens). The effects of the incorporated beads/spheres on the pumpability (viscosity) and the unit weight of the cementitious material were also investigated.
- *Laboratory Experiments Using Foam as the Top Portion of Specimens*
  Using foam as the top portion, unbagged cylindrical specimens were prepared to study the effect of a highly deformable and ductile layer on the mechanical behavior (peak strength, strain at peak strength, and residual strength) of the specimens.
- Laboratory Experiments on Bagged Specimens Containing Internal Reinforcements
  Bagged specimens containing internal layers of reinforcing fibers were prepared to evaluate the effect of internal reinforcements on the mechanical behavior (peak strength, strain at peak strength, and residual strength) of the specimens.

The major findings are: (1) Several types of extremely light, highly compressible, micron-sized beads/spheres were identified. Among them, hollow glass spheres (HGSs) and thermoplastic microspheres (TMs) were selected for detailed laboratory evaluation. (2) The incorporation of HGSs or TMs increases the viscosity of Stream 1 and decreases the unit weight of the specimens. Both HGSs and TMs successfully migrate upward, forming a low-density, highly compressible top layer. The thickness of this top layer increases with increasing HGS or TM content. However, the peak strength of the specimens decreases as the TM or HGS content increases, possibly because some of the HGSs or TMs remain within the lower cementitious material and adversely affect its curing and strength development. Despite this reduction in peak strength, the strain at peak strength increases (i.e., the specimens become more ductile) and the residual strength is higher when more HGSs or TMs are used, both of which are beneficial to the performance of PRSs. (3) Using foam as the top portion of unbagged specimens does not reduce the peak strength because the foam does not affect the matrix integrity or mechanical properties of the lower cementitious material. Furthermore, the strain at peak strength increases significantly (i.e., the specimens become substantially more ductile) as the foam thickness increases, which is beneficial for improving PRS performance. And (4) Bagged specimens containing internal reinforcements exhibited enhanced mechanical performance, including increased peak strength, strain at peak strength, and residual strength.

The use of HGSs or TMs can form a highly deformable top layer but results in a reduction in peak strength. Using foam as the top portion can effectively improve the ductility of pumpable roof supports without adversely affecting their peak strength; however, injecting foam into crib bags under field conditions may be challenging. In this regard, internal reinforcement appears to be a practical and effective approach for enhancing PRS performance. For practical implementation, it is recommended that full-scale demonstrations be conducted by producing and testing full-size PRSs containing internal reinforcements.

2.0 Problem Statement and Objective

2.1. Problem Statement

Pumpable roof supports (PRSs) are increasingly used in underground mines to prevent ground falls because of their advantages in terms of installation, particularly in areas that are difficult to access. A major constituent of PRSs is the cementitious material. In current practice, the most commonly used PRS cementitious material is Portland cement/fly ash (PC/FA)-based grout. However, PC/FA-based PRSs have several limitations, including: (1) the cementitious material can deteriorate significantly when exposed to air, reducing support strength and adversely affecting mine safety, and (2) the peak and residual bearing capacities and the displacement required to reach peak bearing capacity are relatively low. To ensure satisfactory performance of PC/FA-based pumpable supports, it is critically important to minimize or overcome these problems.

In the proof-of-concept project AFC 518-24 completed in 2019, we successfully developed a new hybrid geopolymer/biopolymer (GP/BP) cementitious material for pumpable roof supports. The hybrid GP/BP cementitious material is stable and does not degrade when exposed to air. In addition, the hybrid GP/BP-based pumpable supports have substantially higher peak and residual bearing capacities than the PC/FA-based pumpable supports. These advantages have been successfully demonstrated and validated in the full-scale testing conducted at the NIOSH Mine Roof Simulator (MRS) Laboratory under the follow-up project AFC518SP-94. However, similar to PC/FA-based pumpable supports, hybrid GP/BP-based pumpable supports remain relatively stiff, meaning that the displacement required to reach peak bearing capacity is still limited.

2.2. Objective

The major objective of this research project is to further enhance the performance of pumpable roof supports (PRSs) by increasing their ductility while maintaining their peak and residual bearing capacities. To achieve this objective, the research has focused on the following major tasks:

- *Identification of Extremely Light, Highly Compressible, Micro-Sized Beads/Spheres*
  An extensive search was conducted to identify extremely light, highly compressible, micron-sized beads/spheres that can be incorporated into cementitious materials to form PRSs consisting of a highly deformable and ductile upper portion and a strong lower portion.
- *Laboratory Experiments Using Extremely Light, Highly Compressible, Micro-Sized Beads/Spheres as Additives*
  Using two types of extremely light, highly compressible, micron-sized beads/spheres as additives, both unbagged and bagged cylindrical specimens were prepared to study the effects of incorporated beads/spheres on the mechanical behavior (peak strength, strain at peak strength, and residual strength) of the cementitious material itself (unbagged specimens) and the pumpable support system (bagged specimens). The effects of the

incorporated beads/spheres on the pumpability (viscosity) and the unit weight of the cementitious material were also investigated.

- *Laboratory Experiments Using Foam as the Top Portion of Specimens*
  Using foam as the top portion, unbagged cylindrical specimens were prepared to study the effect of a highly deformable and ductile layer on the mechanical behavior (peak strength, strain at peak strength, and residual strength) of the specimens.
- *Laboratory Experiments on Bagged Specimens Containing Internal Reinforcements*
  Bagged specimens containing internal layers of reinforcing fibers were prepared to evaluate the effect of internal reinforcements on the mechanical behavior (peak strength, strain at peak strength, and residual strength) of the specimens.

3.0 Research Approach

To fulfill the objective of the project, extensive efforts involving four main tasks were pursued as detailed below.

3.1. Identification of Extremely Light, Highly Compressible, Micro-Sized Beads/ Spheres (Task 1)

An extensive search was conducted to identify extremely light, highly compressible, micron-sized beads/spheres that can be incorporated into cementitious materials to form PRSs consisting of a highly deformable and ductile upper portion and a strong lower portion. It was hypothesized that, after incorporating these beads/spheres into one of the two pumpable streams and pumping both streams into a crib bag, the beads/spheres would migrate upward due to buoyancy and accumulate near the top of the grout column within the crib bag. After the crib bag is fully grouted, the beads/spheres are expected to be concentrated in the upper portion of the support. As a results, after curing, the PRS would consist of two distinct portions: (1) an upper portion containing the beads/spheres and exhibiting high compressibility and ductility, and (2) a lower portion containing little or no beads/spheres and retaining the strength of the original cement material. By creating these two functional zones within a single crib bag, the PRS is expected to exhibit not only high peak and residual bearing capacities but also enhanced ductility, characterized by a larger displacement at peak bearing capacity. Such a combination of strength and deformability would provide the desired performance characteristics for PRSs (Fig. 1). The details of this task are provided in Appendix 1.

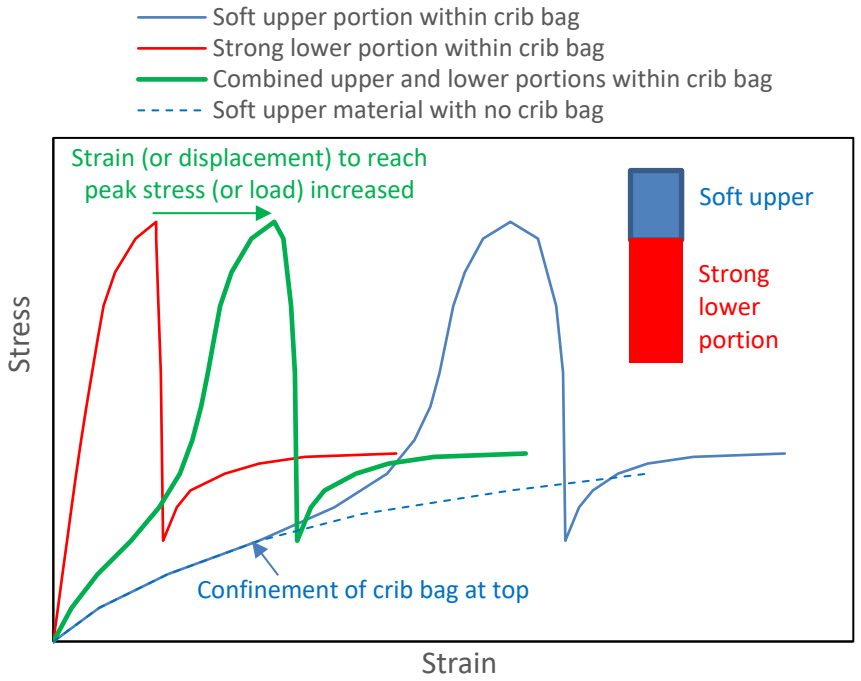


Fig. 1: Schematic showing the design concept of using soft upper portion to increase the strain (displacement) required to reach the peak strength of pumpable roof supports.

3.2. Laboratory Experiments Using Extremely Light, Highly Compressible, Micro -Sized Beads/Spheres as Additives (Task 2)

Using two identified types of extremely light, highly compressible, micron-sized beads/spheres, namely hollow glass spheres (HGSs) and thermoplastic microspheres (TMs), as additives, both unbagged and bagged cylindrical specimens (38.1 mm in diameter and 76.2 mm in height) were prepared to study the effects of incorporated beads/spheres on the mechanical behavior (peak strength, strain at peak strength, and residual strength) of the cementitious material itself (unbagged specimens) and the pumpable support system (bagged specimens). The effects of incorporated beads/spheres on the pumpability (viscosity) and unit weight of the cementitious material were also investigated. Details of this task are provided in Appendix 2.

3.3. Laboratory Experiments Using Foam as Top Portion of Specimens (Task 3)

Since some of the extremely light, highly compressible, micron-sized beads/spheres may remain within the lower cementitious material and adversely affect its mechanical performance, foam was also evaluated as an alternative material for the upper portion of the specimens. Unbagged cylindrical specimens were prepared to investigate the effect of a highly deformable and ductile upper layer on the mechanical behavior (peak strength, strain at peak strength, and residual strength) of the specimens. Details of this task are provided in Appendix 3.

3.4. Laboratory Experiments on Bagged Specimens Containing Internal Reinforcements (Task 4)

Although using foam as the top portion can effectively improve the ductility of PRSs without adversely affecting their peak strength, its field implementation may be challenging because foam would require a separate pumping and injection system. In this regard, bagged specimens containing internal layers of reinforcing fibers were prepared to evaluate the effect of internal reinforcements on the mechanical behavior (peak strength, strain at peak strength, and residual strength) of the specimens (Fig. 2). The fiber reinforcement nets (Fig. 2b) are positioned within the crib bag at predetermined vertical spacings and connected by flexible strings extending from the bottom to the top of the bag (Fig. 2a). When the bag is collapsed prior to installation, the internal reinforcement layers remain stacked in a compact arrangement, thereby facilitating transportation and handling. As the bag is suspended from the mine roof, the reinforcement layers spread apart along the connecting strings while maintaining the specified vertical spacing. Afterward, the grout is pumped into the bag in the same manner as conventional PRS installation to form the support. The details of this task are provided in Appendix 4.

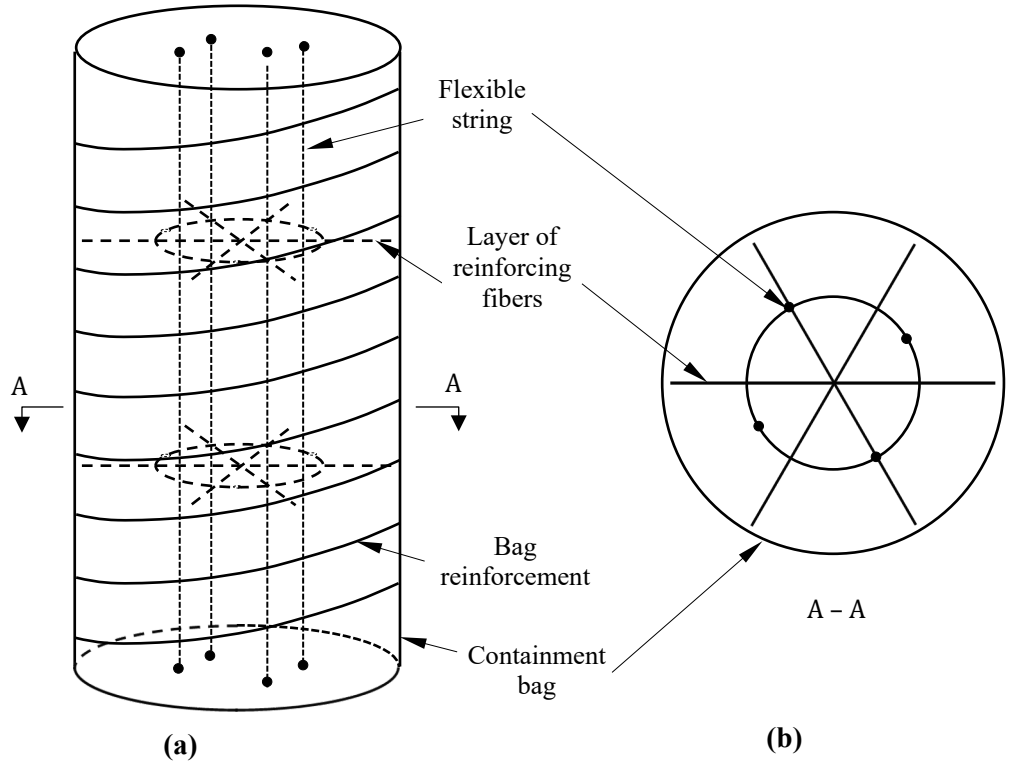


Fig. 2: (a) A confinement bag for PRS containing layers of internal reinforcement nets; and (b) A cross-section showing the internal reinforcement net.

4.0 Research Findings and Accomplishments

4.1. Research Findings

Based on the extensive efforts in this research project, the major findings are summarized below.

4.1.1. Identification of Extremely Light, Highly Compressible, Micro-Sized Beads/Spheres

- There are different types of extremely light, highly compressible, micron-sized beads/spheres. Three candidate materials that can be potentially used to produce strong and ductile high-performance PRSs have been identified: hollow glass spheres (HGSs), Styrofoam filler beads (SFBs), and thermoplastic microspheres (TMs). The HGSs have a diameter of 1–140 μm and a density of 150 kg/m^3. The SFBs have a diameter of approximately 1.5 mm or smaller and an apparent density of 8–15 kg/m^3. And the TMs have a particle size from 13–95 μm and a density as low as 25 kg/m^3 (see Appendix 1).
- Based on their lower densities, the SFBs and TMs are expected to migrate upward more readily than the HGSs and, therefore, may be more effective in forming a low-density, highly compressible upper layer within a crib bag. However, factors such as particle surface characteristics and interactions with the fresh cementitious material must also be considered when evaluating their effectiveness.

4.1.2. Laboratory Experiments Using Extremely Light, Highly Compressible, Micro -Sized Beads/Spheres as Additives

- The viscosity of Stream 1 increased as the HGS or TM content increased, and the increase was more pronounced for TMs. This behavior is attributed to the smoother and harder surfaces of HGSs compared to TMs, which facilitate the movement of surrounding material components and result in less resistance to flow.
- The unit weight of the specimens decreased with increasing HGS or TM content because both materials have substantially lower densities than the premixed PC/FA cement. The reduction in unit weight was more pronounced for TMs because their density is considerably lower than that of HGSs.
- Both HGSs and TMs successfully migrated upward to form a low-density, highly compressible upper layer within the specimens, and the thickness of this layer increased with increasing HGS or TM content. In addition, the upper layer formed by TMs was slightly thicker than that formed by HGSs.
- The peak uniaxial compressive strength (UCS) of the specimens decreased as the HGS or TM content increased. This reduction is likely because some HGSs or TMs remained within the lower cementitious material instead of migrating upward, thereby adversely affecting cement hydration and strength development. The reduction in peak UCS was substantially smaller for bagged specimens than for unbagged specimens, which is encouraging because PRSs are used in a bagged configuration in practice. However, the strain at peak UCS increased (i.e., the specimens became more ductile), and the residual

strength also increased as the HGS or TM content increased, both of which are beneficial to PRS performance

- Furthermore, specimens containing HGSs, whether bagged or unbagged, generally exhibited slightly higher peak UCS values, greater strain at peak UCS, and higher residual strength than specimens containing TMs. This difference may be attributed to the greater adverse effects of TMs retained within the cementitious matrix on its mechanical behavior.

4.1.3. Laboratory Experiments Using Foam as Top Portion of Specimens

- Using foam as the top portion of unbagged specimens did not affect the peak UCS because the foam itself did not affect the matrix integrity or mechanical properties of the underlying cementitious material. However, the strain at the peak UCS increased significantly (i.e., the specimen became substantially more ductile) when the thickness of the foam layer increased, which is beneficial to the performance of PRSs. This improvement is primarily attributable to the large compressibility and deformation capacity of the foam under relatively low applied loads.

4.1.4. Laboratory Experiments on Bagged Specimens Containing Internal Reinforcements

- Internal reinforcement progressively increased the peak strength of the PRS specimens. The average peak strength increased from 3.85 MPa for the No Reinforcement Layer (No RL) specimens to 4.80 MPa for the Three Reinforcement Layer (Three RL) specimens, corresponding to an increase of 24.7%. In addition, compared with the No RL specimens, the strain at the peak stress for the Three RL specimens increased by 65.2%, indicating that the reinforced specimens accommodated significantly larger deformation before reaching their maximum load-bearing capacity.
- The internal reinforcement substantially improved the post-peak stability of the PRS specimens. The number of load-shed events recorded up to 8% strain decreased from five for the No RL specimens to one for the Three RL specimens. This improvement is attributed to the confinement-restoration mechanism provided by the internal reinforcement layers. The internal reinforcement layers acted as localized restraints that limited lateral dilation, reduced crack progression, and retained the fractured cementitious infill core within the containment bag.
- The improvement in residual load-bearing capacity was more pronounced. At 8% strain, the average residual stress increased from 2.51 MPa for the No RL specimens to 4.27 MPa for the Three RL specimens, representing an increase of 70.1%. The improvement is attributed to the ability of the internal reinforcement layers to provide additional lateral restraint at multiple elevations along the specimen height, retaining and consolidating the fractured cementitious infill core and reducing the exclusive dependence of the post-peak response on the outer confinement bag and ties.

4.2. Accomplishments

This research project has achieved the following major accomplishments:

1) Extremely light, highly compressible, micron-sized beads/spheres have been identified as potential additives for producing strong, ductile, and high-performance pumpable roof supports (PRSs).
2) Systematic laboratory investigations were conducted to evaluate the effects of extremely light, highly compressible, micron-sized beads/spheres on the performance of PRSs. The results demonstrated that the incorporation of these beads/spheres enhances the ductility of PRSs but may reduce their peak strength.
3) The study demonstrated the effectiveness of using foam as the upper portion of specimens to increase ductility while maintaining peak uniaxial compressive strength (UCS). However, field implementation of this approach may be challenging because it would require a separate pumping and injection system for the foam material.
4) The study successfully demonstrated the potential of internal reinforcement as a practical and effective strategy for enhancing the performance of PRSs. Specifically, internal reinforcement increased the peak strength, strain at peak strength, and residual strength of the specimens, while also improving their post-peak stability and load-bearing capacity.

5.0 Publication Record and Dissemination Efforts

So far, one refereed journal paper has been published:

- Khawaja, S. A., Barczak, T. M., and Zhang, L. (2026). "A Novel Internal Reinforcement Approach for Improving the Performance of Pumpable Roof Supports." *Mining, Metallurgy & Exploration*, https://doi.org/10.1007/s42461-026-01721-x.

In addition, efforts are underway to facilitate technology transfer and commercialization of the research outcomes. The research team is currently working with the Technology Transfer Department at the University of Arizona to pursue patent protection and commercialization opportunities for the novel internal reinforcement technology, with the goal of advancing its adoption and implementation in practical mining applications.

6.0 Conclusions and Impact Assessment

Based on the systematic study, the following conclusions can be drawn:

1) Extremely light, highly compressible, micron-sized beads/spheres, including hollow glass spheres (HGSs) and thermoplastic microspheres (TMs), can successfully migrate upward within the cementitious material and form a low-density, highly compressible upper layer, thereby increasing the ductility of pumpable roof supports (PRSs)
2) The incorporation of HGSs or TMs enhances the ductility and residual load-bearing capacity of PRSs; however, it may reduce peak strength because a portion of the beads/spheres remains within the lower cementitious material and adversely affects its strength development
3) Using foam as the upper portion of the support is highly effective for increasing ductility while maintaining peak strength because the foam does not compromise the integrity or mechanical properties of the underlying cementitious material. However, field implementation may be challenging due to the need for a separate pumping and injection system
4) Internal reinforcement provides a practical and effective approach for improving PRS performance. The incorporation of internal reinforcement layers increases peak strength, strain at peak strength, residual strength, and post-peak stability, making PRSs more capable of sustaining large ground movements while maintaining load-bearing capacity.

The research has identified and evaluated several innovative approaches for enhancing the performance of PRSs and has successfully demonstrated the effectiveness of internal reinforcement as a practical solution for improving both strength and ductility. The findings provide valuable scientific and engineering knowledge for the development of next-generation high-performance PRSs. In addition, the project has resulted in a refereed journal publication and has created opportunities for technology transfer, patent development, and future commercialization. The findings of this research are expected to improve ground control practices, increase support reliability under demanding underground conditions, and reduce the risk of roof falls and support failures, thereby contributing to improved safety and productivity in underground mining operations.

7.0 Recommendations for Future Work

The study successfully demonstrated the potential of internal reinforcement as a practical and effective strategy for enhancing the performance of PRSs. Specifically, internal reinforcement increased the peak strength, strain at peak strength, and residual strength of the specimens, while also improving their post-peak stability and load-bearing capacity. For practical implementation, it is recommended that full-scale demonstrations be conducted by producing and testing full-size PRSs containing internal reinforcements.

8.0 Appendices

Appendix 1: Identification of Extremely Light, Highly Compressible, Micro-Sized Beads/Spheres

Extensive searches were conducted to identify extremely light, highly compressible, micron-sized beads or spheres. Three types of such beads/spheres were identified and evaluated for potential use in pumpable roof supports (PRSs), as described below.

A1.1 Hollow Glass Spheres (HGSs)

The hollow glass spheres (GL0237B/1-140) from MO SCI, LLC (https://www.mo-sci.com/) have a diameter of 1–140 μm, a density of 150 kg/m^3, and a crush strength of 300 psi (2.07 MPa). Fig. A1-1 shows 4 lbs of hollow glass spheres in a 5-gallon bucket.



Fig. A1-1: 4 lbs of hollow glass spheres in a 5-gallon bucket (from https://www.mo-sci.com/).

A1.2 Styrofoam Filler Beads (SFBs)

The Styrofoam filler beads with a diameter of approximately 1.5 mm or smaller (Fig. A1-2) have an apparent density of 8–15 kg/m^3. It is expected that the extremely low density of the Styrofoam filler beads will make them to easily move to the top of the grout within the crib bag. However, the Styrofoam filler beads may absorb water during the mixing and pumping process, affecting the capability of the beads to move upward and the curing of the cementitious material. These effects need to be studied systematically.



Fig. A1-2: Styrofoam filler beads (from https://www.etsy.com/).

A1.3 Thermoplastic Microspheres (TMs)

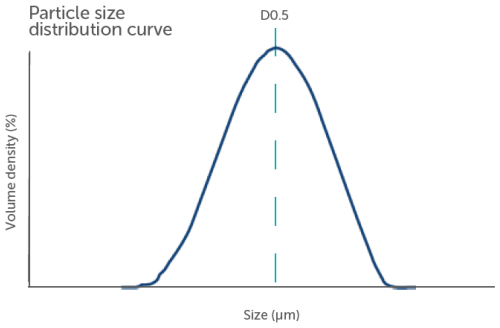
The Expancel® thermoplastic microspheres from Nouryon (https://www.nouryon.com/) have a particle size from 13–95 μm and a density as low as 25 kg/m^3 (see Table A1-1). The Expancel® thermoplastic microspheres have been used as lightweight fillers for different applications.

Table A1-1: Expancel® thermoplastic microspheres from Nouryon (from https://www.nouryon.com/).

Expancel® grade	Particle size D(0.5) [1] µm	True density [2] kg/m^3	Solvent resistance [3]
920 DET 20 d40	13–30	36–44	5
920 DE 40 d30	35–55	27–33	5
920 DET 40 d25	30–60	22–28	5
920 DE 80 d30	55–85	27–33	5
HP92 DET 80 d45	60–85	42–50	5
043 DET 80 d20	60–95	17–23	4

1) Particle size: measured by laser diffraction; Low Angle Laser Light Scattering (LALLS). D(0.5) = average particle size.
More information: "Particle size of Expancel® Microspheres".
2) Density: measured by pycnometer to ensure the specified density of expanded microspheres.
More information: "Density measurements of Expancel® Microspheres".
3) Solvent resistance: The microspheres are immersed in pure, liquid chemical or water solution of the chemical and tumbled for 24 h at 40°C (104°F). After drying the density is measured, and any discoloration is visually observed.
More information: "Chemical resistance of Expancel® Microspheres".

Solvent resistance rating:
5 = no unfavorable effects expected
4 = special care needed if mixed for prolonged periods or at elevated temperatures
3 = poor chemical resistance



Appendix 2: Laboratory Experiments Using Extremely Light, Highly Compressible, Micro-Sized Beads/Spheres as an Additive

The premixed PC/FA cement (the actual PC/FA based cementitious material used in practice) received from a pumpable roof support installer was used as the base cementitious material. Table A2-1 shows the composition of the PC/FA based cementitious material specimens containing different amounts of HGSs or TMs.

Table A2-1 Composition of PC/FA based cementitious material specimens containing different amounts of hollow glass spheres (HGSs) or thermoplastic microspheres (TMs).

HGSs or TMs (vol.%)	Stream I			Stream II	
	Premixed PC/FA cement (gr)	Water (gr)	HGSs [or TMs] (gr)	Sodium Silicate (ml)	Water (ml)
0	500	534	0 [0]	300	1176
35	450	534	50 [10.90]	300	1176
50	425	534	75 [16.35]	300	1176
75	400	534	100 [21.80]	300	1176

As can be seen in Table A2-1, the PC/FA based cementitious material specimens contain two separate pumpable streams: stream 1 composed of premixed PC/FA cement, water and HGSs or TMs, and stream 2 containing sodium silicate and water. To prepare the first stream, the premixed PC/FA cement was first mixed with the TMs if TMs were used and then with water to obtain a homogeneous slurry. To prepare the second stream, sodium silicate and water were mixed thoroughly to ensure homogeneity.

The viscosity (pumpability) test was performed on stream 1 prepared at different contents of HGSs or TMs using a Fann model 35A viscometer (Fig. A2-1). Since stream 2 is simply a sodium silicate solution and can be easily pumped, no rheology test was performed on it. To this end, the slurry is confined between two concentric cylinders with different radii, and one of the cylinders rotates at a certain speed. In this model, the slurry in the large radius recipient is sheared between the outer sleeve (rotor) and the inner cylinder (bob) connected to a torque measuring device. The torque required to rotate the bob is measured by the viscometer. By changing the rotational speed (3, 6, 100, 200, 300, and 600 rpm), several viscosity ranges can be measured. This test was performed in accordance with API Spec 10's instructions. In this regard, the first torque reading was done after one minute of shearing the slurry at the highest rotational speed, and then the rotational speed was sequentially decreased to the lower rotational velocity and the corresponding torque reading was done after 20 seconds of rotation at each rotational speed. The equations and constants provided by the viscometer manufacturer were used for calculating the viscosity.



Fig. A2-1: Viscometer Fann model 35A.

Figure A2-2 shows the viscosity of stream 1 at different contents of HGSs or TMs. As can be seen, the viscosity of stream 1 increases significantly as more HGSs or TMs are used, and the increase is more significant when TMs are used. This is because HGSs have smoother and harder surfaces compared to TMs, which allows other material components to move more easily around the HGSs. According to the literature, a cementitious material with a viscosity below 300 cP is considered pumpable. Therefore, to ensure good pumpability of stream 1, a HGSs or TMs content of no more than 50 vol.% was used in the next studies. Again, stream 2 is simply a non-setting sodium silicate solution and can be easily pumped.

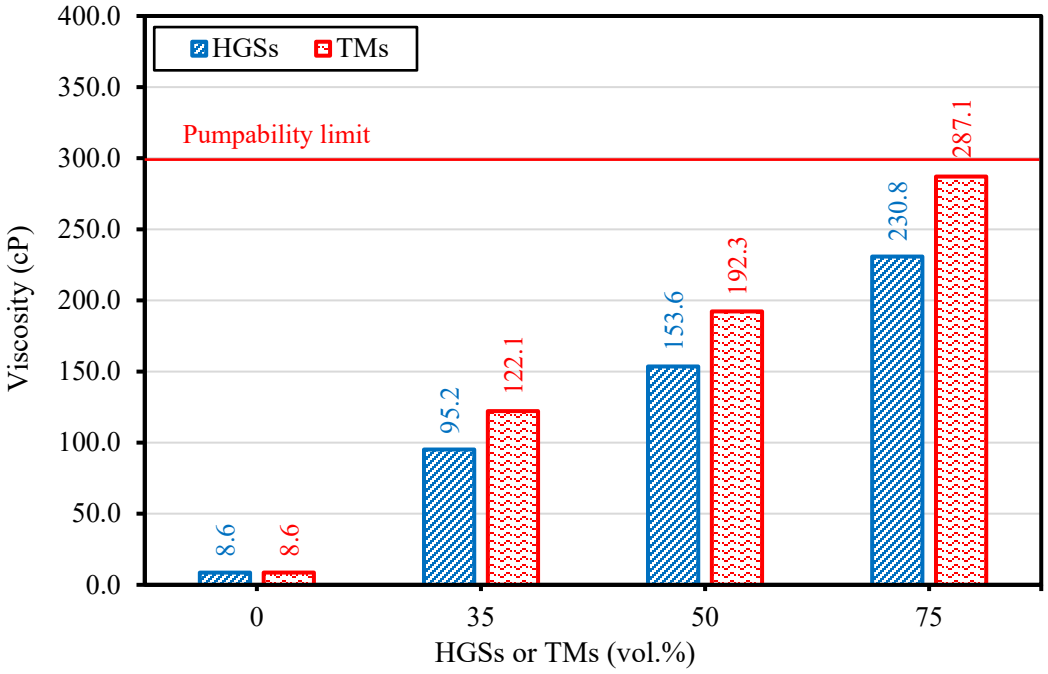


Fig. A2-2: Viscosity of stream 1 containing different amounts of HGSs or TMs.

A2.1 Unbagged Specimens

During this period, unbagged cylindrical specimens containing different amounts of TMs (0, 35, and 50 vol.%) were prepared for uniaxial compression tests. To do that, the two streams were mixed thoroughly and then poured into cylindrical molds (38.1 mm in diameter and 76.2 mm in height). The molds were placed at room temperature for curing. After 24 hours, the specimens were removed from the molds and fully sealed with plastic sheets. The sealed specimens at different conditions were kept at room temperature for further curing until the test day.

Fig. A2-3 shows the unit weight of the unbagged specimens after 28 days of curing at different HGSs or TMs contents. As expected, the unit weight of the specimens decreases with a higher HGSs or TMs content, and the decrease is more significant when TMs are used. This is simply because the HGSs and TMs both have a much smaller density than the premixed PC/FA cement and TMs are lighter than HGSs.

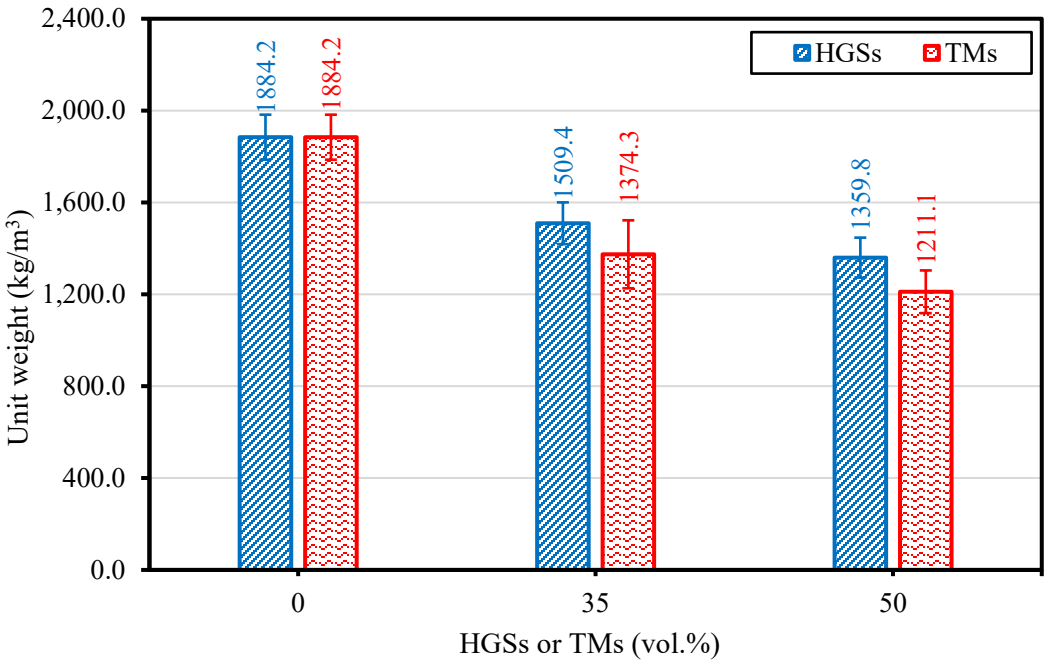


Fig. A2-3: Unit weight of 28 day cured unbagged specimens prepared with premixed PC/FA cement and containing different amounts of HGSs or TMs.

As shown in Fig. A2-4, a thin layer of HGSs or TMs is formed at the top of the specimen when they are used. In addition, the thickness of the top layer increases when more HGSs or TMs are used. Therefore, it can be concluded that the HGSs or TMs did move upward to the top after the two streams were mixed into the molds. Also, under a compressive loading, the top layer is more compressible with larger radial deformation and thus more ductile than the lower part as clearly shown in Fig. A2-4(b). This can be further seen and will be discussed in more detail later.

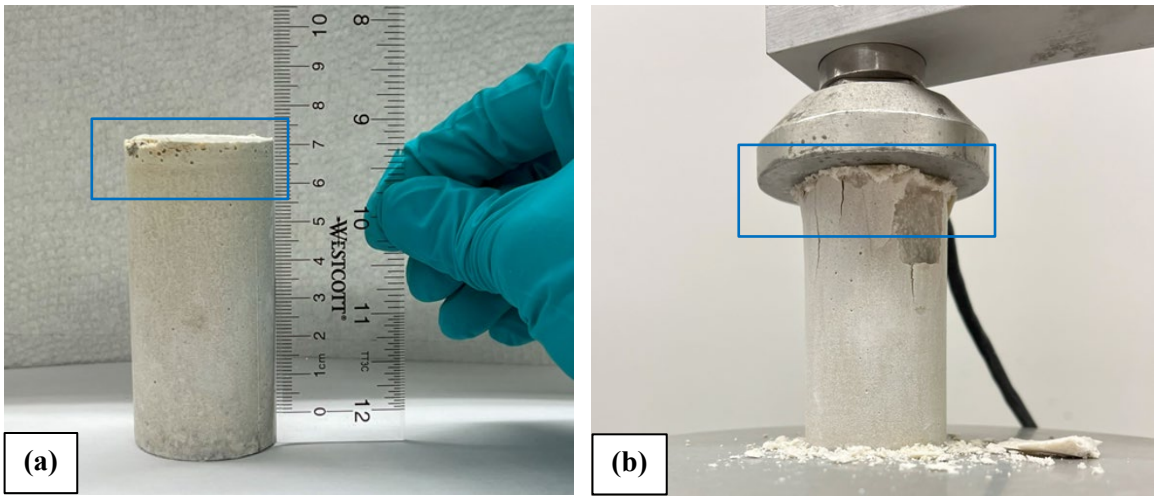


Fig. A2-4: (a) Formed layer of TMs at the top of the specimen, and (b) Compression of the top ductile layer during the UCS test.

However, it appears that not all the HGSs or TMs have moved to the top of the specimen, based on the quantities of HGSs or TMs used and the thickness of the formed top layer. This observation is further supported by comparing the images of the fractured specimens after the UCS test with 0 vol.% and 50 vol.% TMs, respectively (Fig. A2-5). As can be seen, at 50 vol.% of TMs, some TMs were trapped within the specimen. This is possibly because the viscosity of the mortar is high enough to prevent some of the HGSs or TMs from rising. In other words, the internal friction within the mixture counteracts the buoyant forces that try to move the HGSs or the TMs upward.

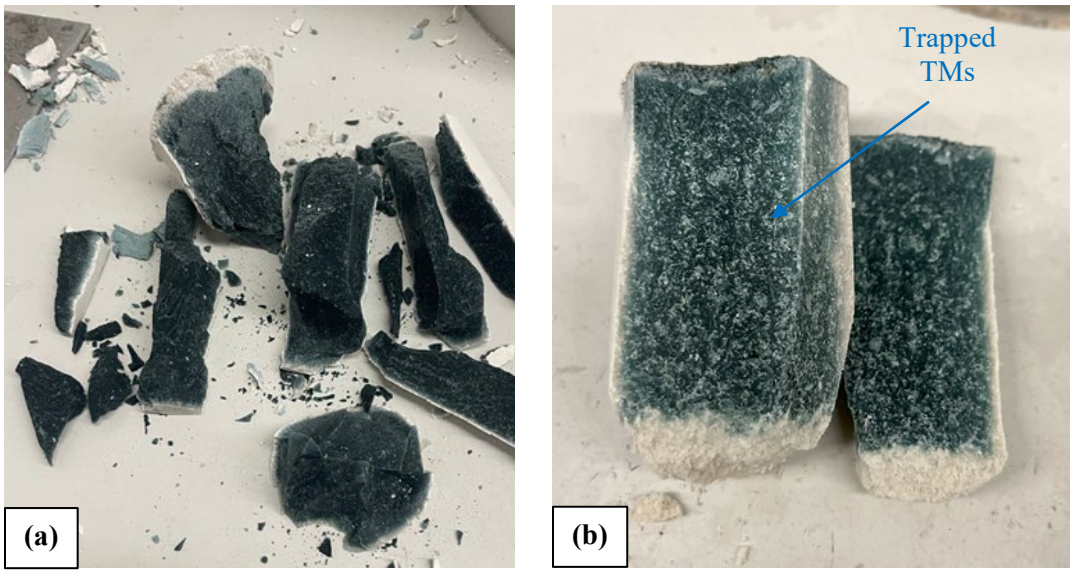


Fig. A2-5: Fractured specimens after UCS test: (a) 0 vol.% TMs, and (b) 50 vol.% TMs.

Fig. A2-6 shows the 28-day cured unbagged specimens at different HGSs or TMs contents before, during and after the uniaxial compression test, which further indicates the formed top layer of HGSs or TMs at different HGSs and TMs contents. When the same volume amount of HGSs or TMs is used, the thickness of the top layer of TMs is slightly greater than that of HGSs, simply because TMs are lighter than HGSs.

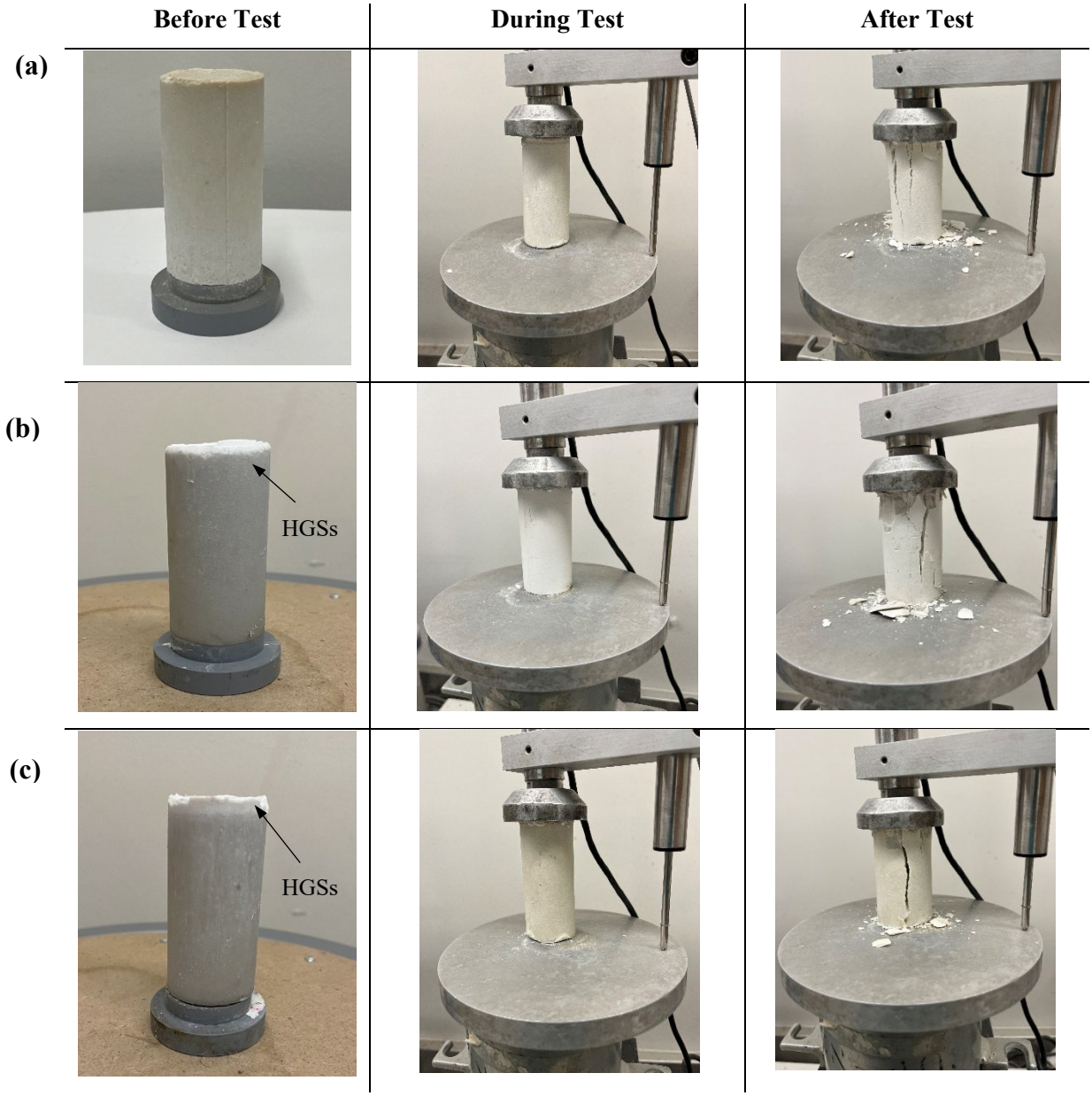


Fig. A2-6/1: Pictures of unbagged specimens prepared with premixed PC/FA cement and containing different amounts of HGSs: (a) 0 vol.%, (b) 35 vol.%, and (c) 50 vol.%.

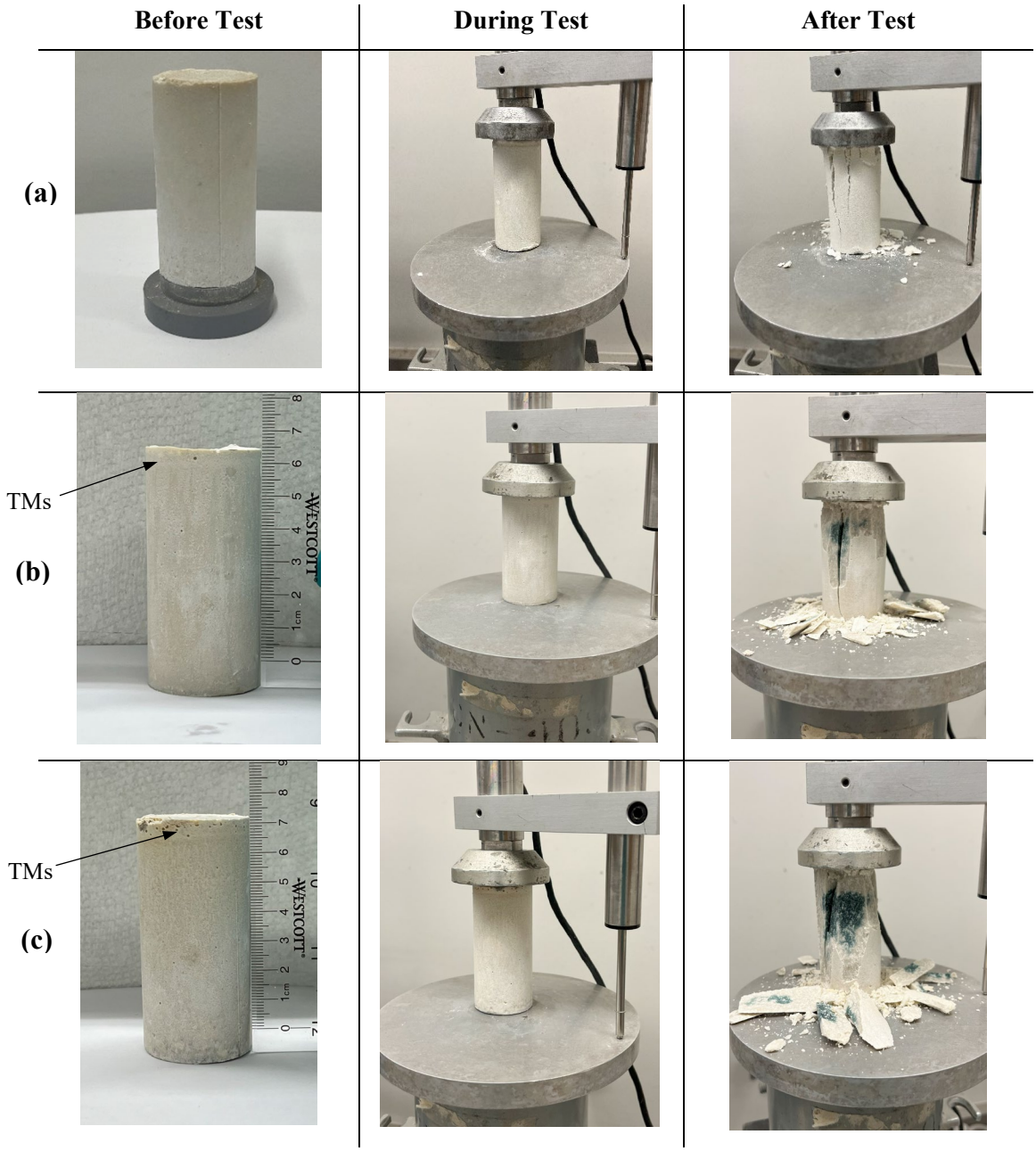


Fig. A2-6/2: Pictures of unbagged specimens prepared with premixed PC/FA cement and containing different amounts of TMs: (a) 0 vol.%, (b) 35 vol.%, and (c) 50 vol.%.

Fig. A2-7 shows the stress-strain curves of the unbagged specimens after 28 days' curing at different HGSs or TMs contents, with the UCS and the strain the peak UCS summarized in Table A2-2. As can be seen, the peak UCS decreased when more HGSs or TMs were used. This is possibly because some of the HGSs or TMs did not move upward to the top but stayed within the cementitious material and adversely affected the curing and strength of the cementitious material – which will be further checked later. However, as expected, the strain at the peak UCS increased (i.e., the specimen became more ductile) and the residual strength

was higher when more HGSs or TMs were used (see Table A2-2) – which is beneficial for the performance of pumpable roof supports. At the same volume amount of HGSs or TMs, the specimens containing HGSs have slightly higher peak UCS, larger strain at the peak UCS, and higher residual strength than those containing TMs. So HGSs are more effective than TMs, possibly because the TMs trapped in the mortar have more adverse effects on the mechanical behavior of the cementitious material.

A2.2 Bagged Specimens

Bagged cylindrical specimens containing different amounts of HGSs or TMs (0, 35, and 50 vol.%) were also prepared for uniaxial compression tests. To do that, we searched and evaluated different types of fabrics – Fig. A2-8 shows four of them. By considering the fabric strength and the ease to prepare the bag (fabric confinement), the fiberglass cloth was used.

By following the procedure as shown in Fig. A2-9, the bag (fabric confinement) within a mold was first prepared. With fabric confinement within the mold, bagged specimens were then produced following the same procedure as that in Section A2.1 for preparing the unbagged specimens.

Fig. A2-10 shows the 28-day cured bagged specimens at different HGSs or TMs contents before, during and after the uniaxial compression test. Due to the confining bag, the thickness of the formed layer of HGSs or TMs at the top of the specimens cannot be seen.

Fig. A2-11 shows the stress-strain curves of the bagged specimens after 28 days' curing at different HGSs or TMs contents, with the peak uniaxial compressive strength (UCS) and the strain the peak UCS summarized in Table A2-3. By comparing Fig. A2-11 with Fig. A2-7 and Table A2-2 with Table A2-3, one can see that the use of bag (fabric confinement) increased both the peak UCS and the strain at the peak UCS significantly, especially when HGSs or TMs were used. This is simply due to the confinement from the bag as clearly shown in Fig. A2-12. Like the unbagged specimens, the peak UCS of the bagged specimens decreased when more HGSs or TMs were used, but the degree of decrease was much smaller – which is good considering that crib bags are used in practice. Again, the decrease of peak UCS with more HGSs or TMs is possibly because some of the HGSs or TMs did not move upward to the top but stayed within the cementitious material and adversely affected the curing and strength of the cementitious material. However, as expected, the strain at the peak UCS increased (i.e., the specimen became more ductile) and the residual strength was higher when more HGSs or TMs were used – which is beneficial for the performance of pumpable roof supports. Also, the HGSs are more effective than the TMs with higher peak UCS, larger strain at the peak UCS, and higher residual strength, possibly because the TMs trapped in the mortar have more adverse effects on the mechanical behavior of the cementitious material.

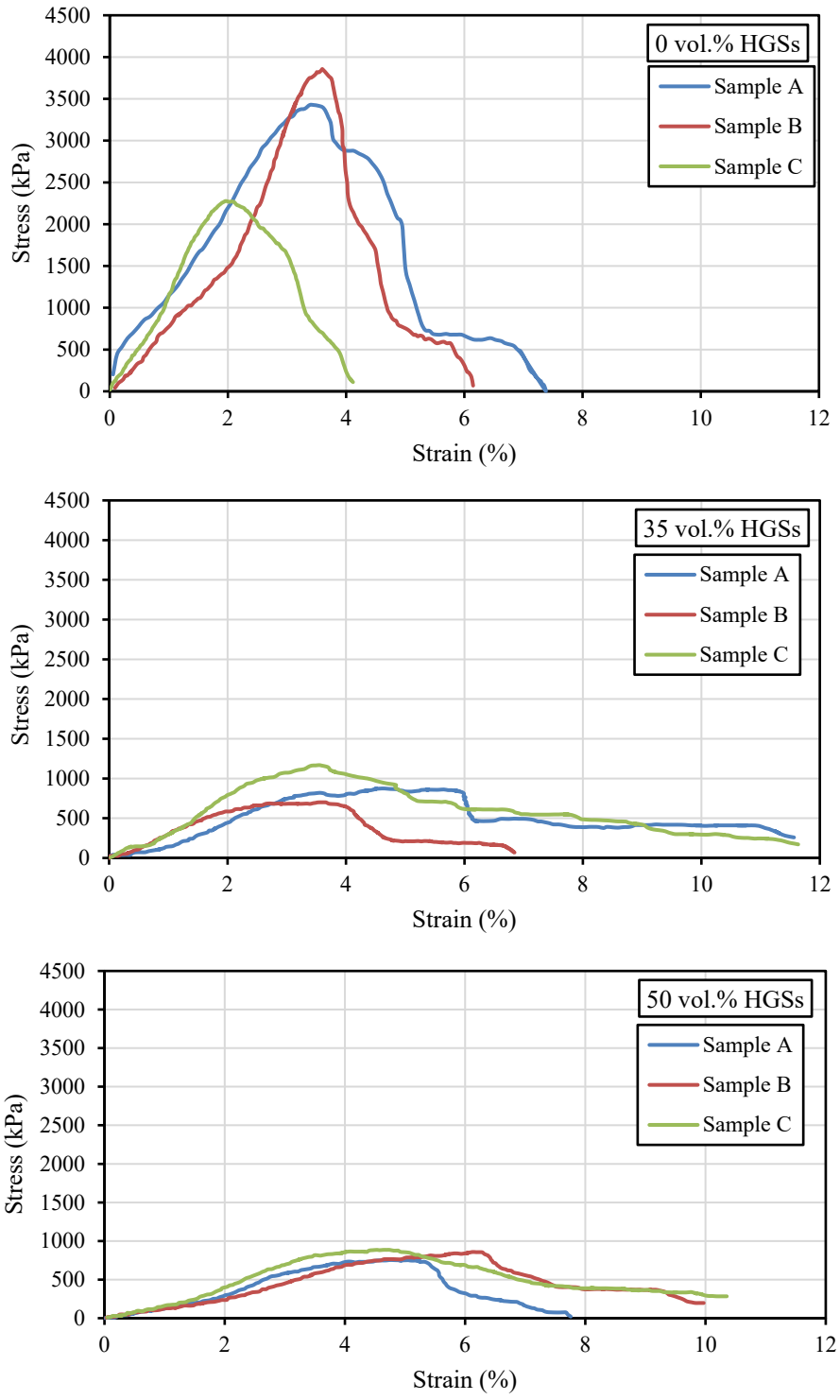


Fig. A2-7/1: Stress-strain curves of unbagged specimens prepared with premixed PC/FA cement and different amounts of HGSs: (a) 0 vol.%, (b) 35 vol.%, and (c) 50 vol.%.

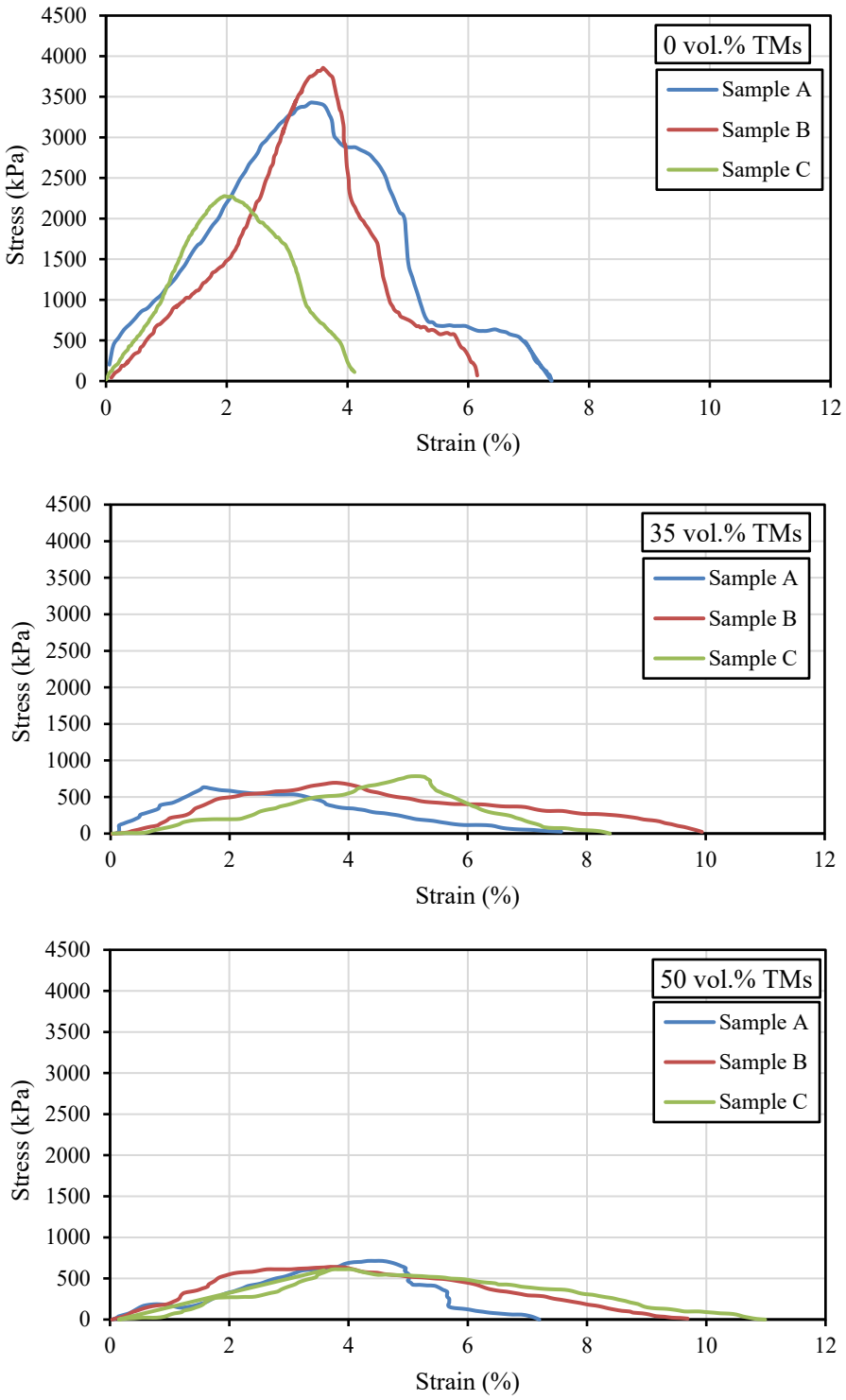


Fig. A2-7/2: Stress-strain curves of unbagged specimens prepared with premixed PC/FA cement and different amounts of TMs: (a) 0 vol.%, (b) 35 vol.%, and (c) 50 vol.%.

Table A2-2: Summary of peak UCS and strain at peak UCS of unbagged specimens containing different amounts of HGSs or TMs.

Specimen	HGSs				TMs			
	Peak UCS (MPa)	Strain at peak UCS (%)	Average peak UCS (MPa)	Average strain at peak UCS (%)	Peak UCS (MPa)	Strain at peak UCS (%)	Average peak UCS (MPa)	Average strain at peak UCS (%)
0 vol.% A	3.417	3.41	3.174	2.94	3.417	3.41	3.174	2.94
0 vol.% B	3.839	3.62			3.839	3.62		
0 vol.% C	2.266	1.81			2.266	1.81		
35 vol.% A	0.875	4.51	0.914	3.88	0.632	1.56	0.702	3.55
35 vol.% B	0.699	3.59			0.695	3.98		
35 vol.% C	1.168	3.54			0.779	5.11		
50 vol.% A	0.751	4.68	0.831	5.09	0.713	4.56	0.655	4.06
50 vol.% B	0.858	6.07			0.641	3.69		
50 vol.% C	0.885	4.52			0.611	3.94		



Fig. A2-8: Different types of fabrics considered: (a) Fiberglass cloth, (b) Glass fiber mesh, (c) Polyester, and (d) Molding fiberglass.



Fig. A2-9: Procedure for preparing fabric confinement within a mold for producing bagged specimens.

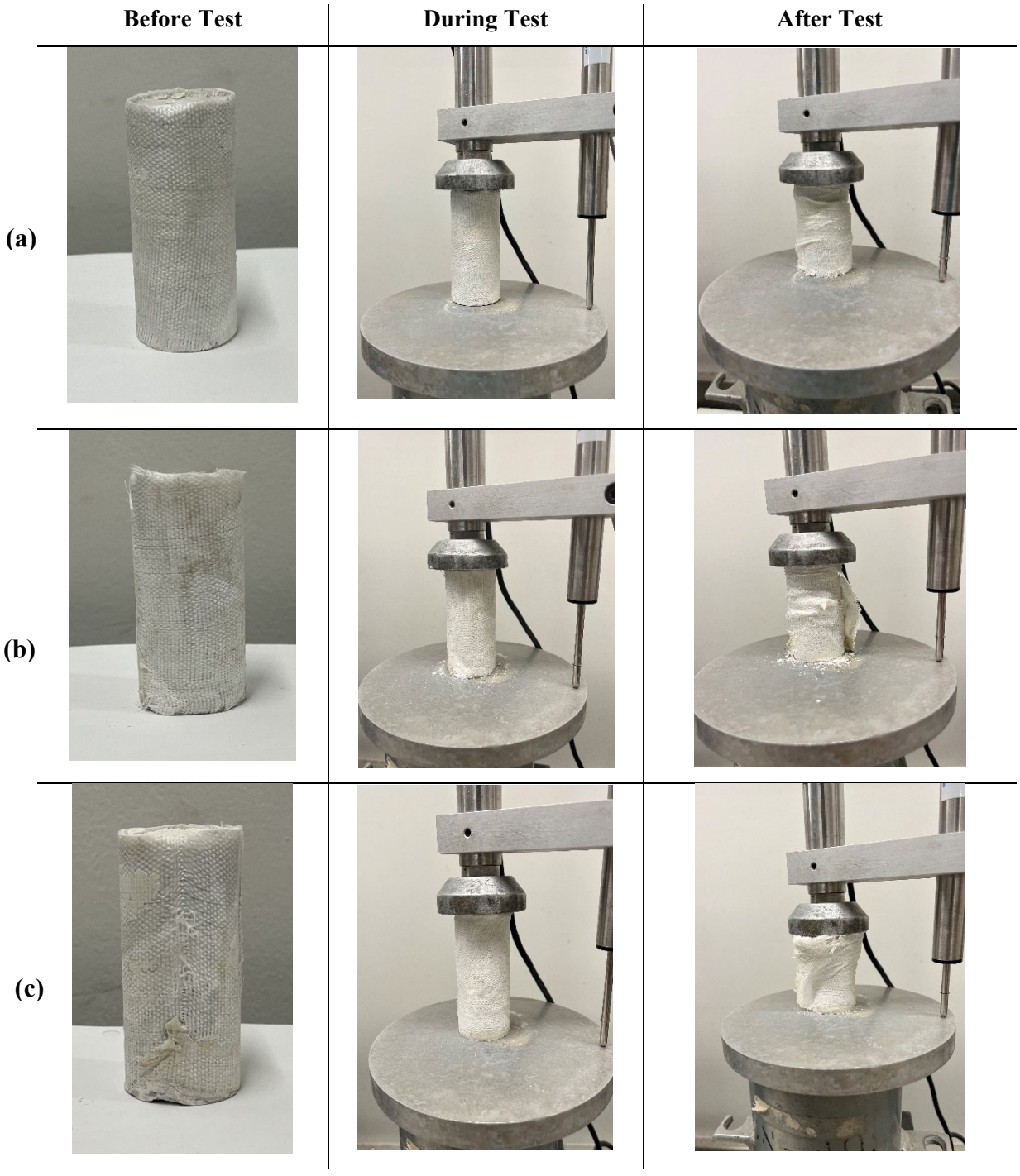


Fig. A2-10/1: Pictures of bagged specimens prepared with premixed PC/FA cement and different amounts of HGSs: (a) 0 vol.%, (b) 35 vol.%, and (c) 50 vol.%.

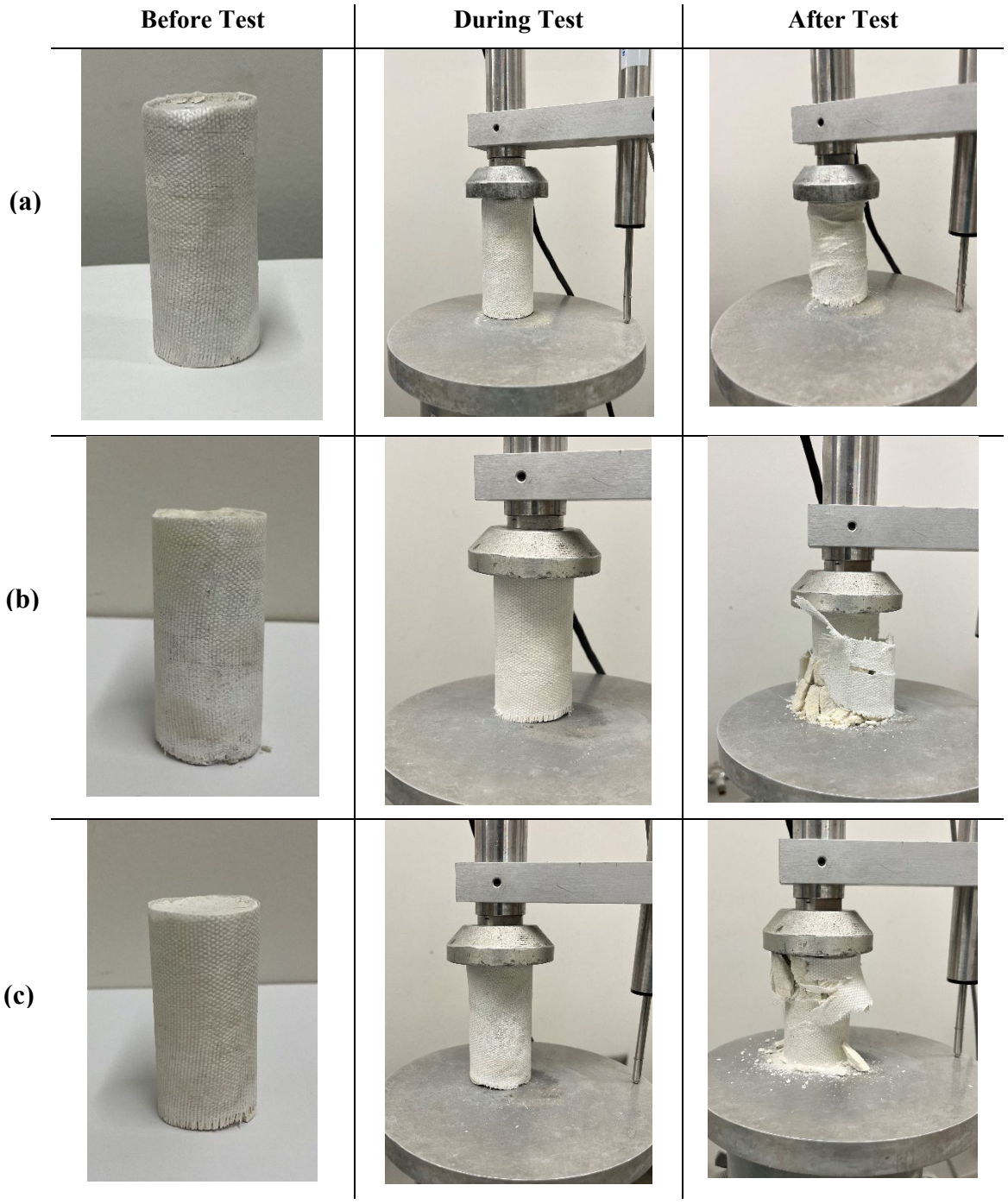


Fig. A2-10/2: Pictures of bagged specimens prepared with premixed PC/FA cement and different amounts of TMs: (a) 0 vol.%, (b) 35 vol.%, and (c) 50 vol.%.

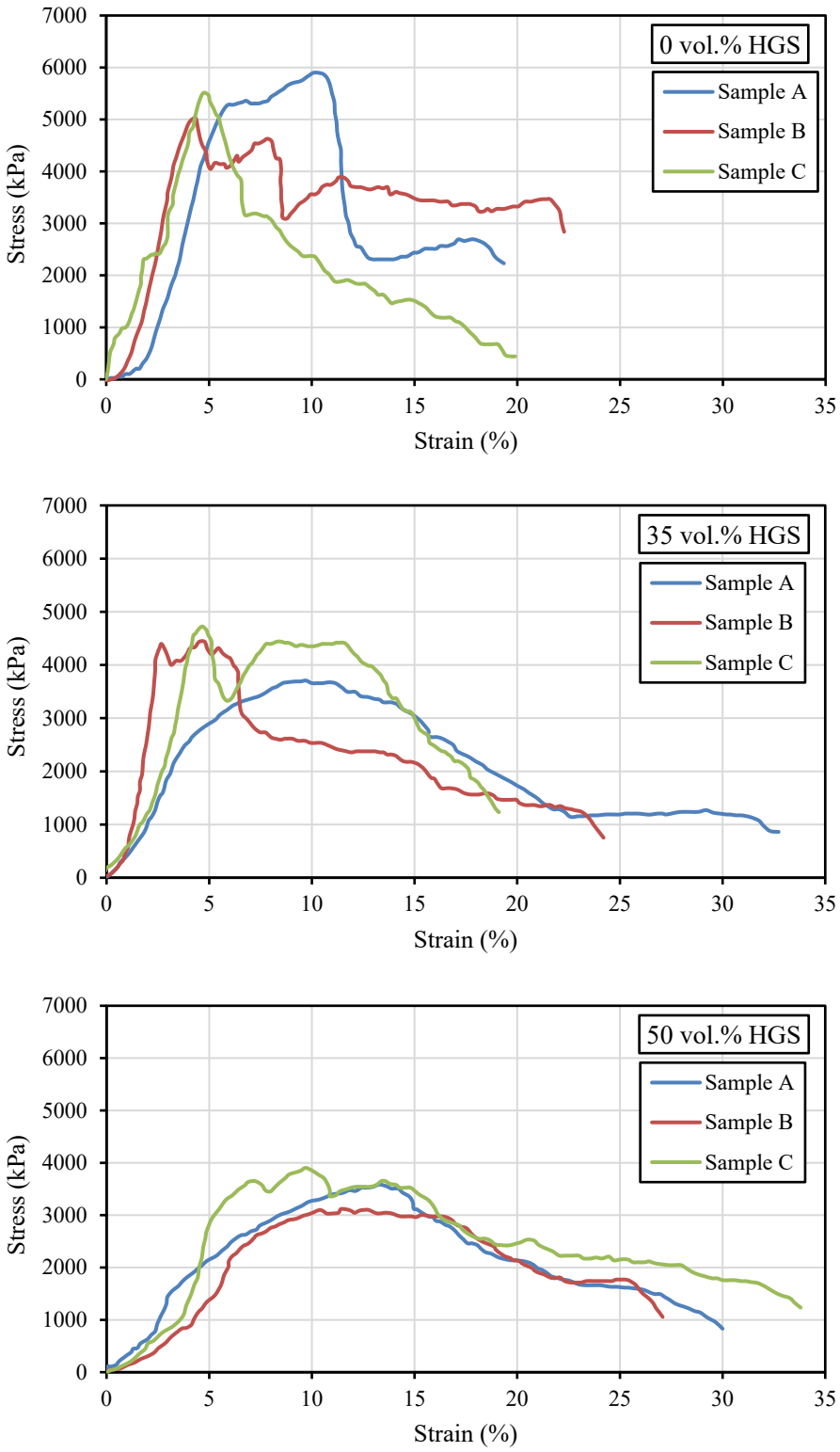


Fig. A2-11/1: Stress-strain curves of bagged specimens prepared with premixed PC/FA cement and different amounts of HGSs: (a) 0 vol.%, (b) 35 vol.%, and (c) 50 vol.%.

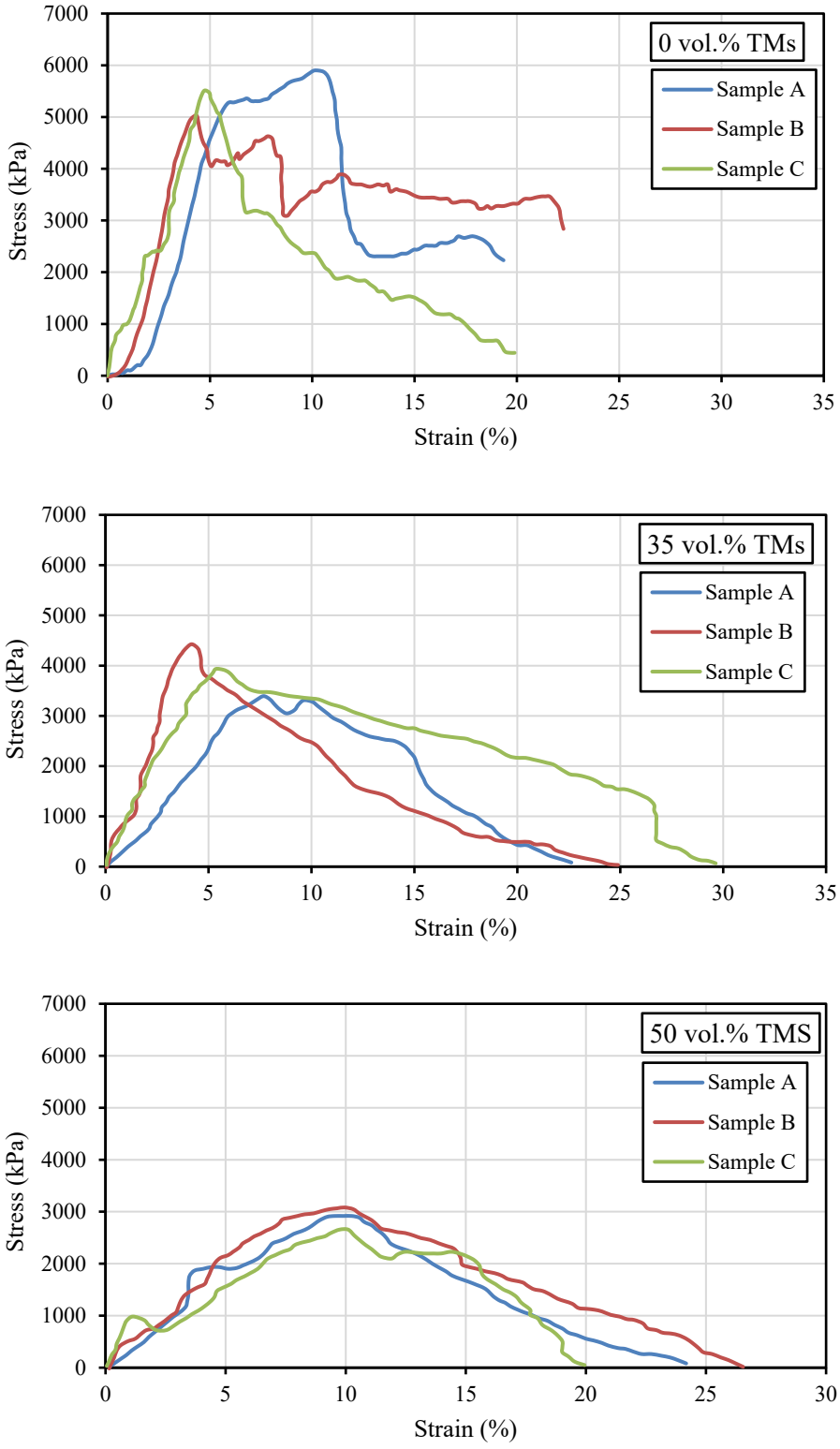


Fig. A2-11/2: Stress-strain curves of bagged specimens prepared with premixed PC/FA cement and different amounts of TMs: (a) 0 vol.%, (b) 35 vol.%, and (c) 50 vol.%.

Table A2-3: Summary of peak UCS and strain at peak UCS of bagged specimens containing different amounts of HGSs or TMs.

Specimen	HGSs				TMs			
	Peak UCS (MPa)	Strain at peak UCS (%)	Average peak UCS (MPa)	Average strain at peak UCS (%)	Peak UCS (MPa)	Strain at peak UCS (%)	Average peak UCS (MPa)	Average strain at peak UCS (%)
0 vol.% A	5.969	10.42	5.44	6.55	5.969	10.42	5.44	6.55
0 vol.% B	5.001	4.12			5.001	4.12		
0 vol.% C	5.465	5.51			5.465	5.51		
35 vol.% A	3.718	9.11	4.29	7.07	3.393	7.68	3.912	5.72
35 vol.% B	4.486	4.58			4.409	4.12		
35 vol.% C	4.681	4.52			3.934	5.36		
50 vol.% A	3.576	13.27	3.54	11.6	2.918	10.25	2.884	10.12
50 vol.% B	3.127	11.55			3.081	10.39		
50 vol.% C	3.920	9.82			2.655	9.74		

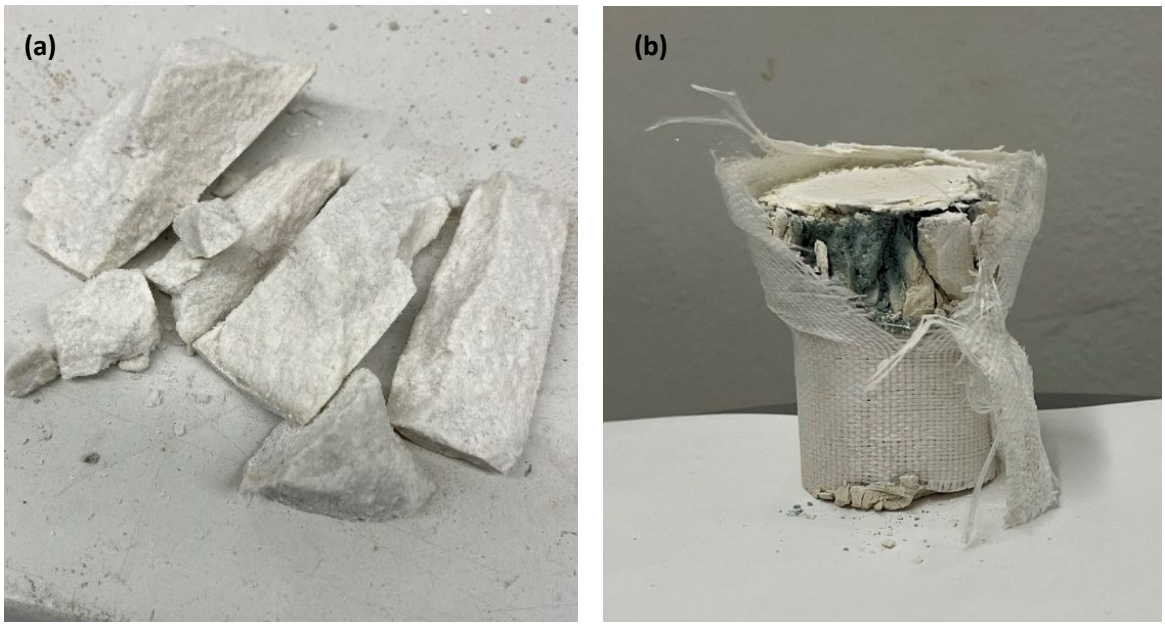


Fig. A2-12: Picture of failed specimens: (a) Unbagged, and (b) Bagged, both at 50 vol.% HGSs.

Appendix 3: Laboratory Experiments Using Foam as Top Portion of Specimens

Since the incorporation of beads/spheres led to a decrease of the peak strength of specimens (see Appendix 2), we prepared unbagged cylindrical specimens by using closed-cell polyethylene foam as the top portion to study the effect of the top highly deformable portion on the mechanical behavior (peak strength, strain at peak strength, etc.) of the specimens. The following presents the results obtained.

Fig. A3-1 shows the 28-day cured unbagged specimens with different heights (0, 10, 20, and 30 ht.%, respectively) of foam as the top portion, before, during and after the uniaxial compression test.

Fig. A3-2 shows the stress-strain curves of the unbagged specimens after 28 days' curing with different heights of foam as the top portion, with the peak UCS and the strain at the peak UCS summarized in Table A3-1. As can be seen, the peak UCS remained relatively consistent, ranging approximately between 2.71 and 3.33 MPa, regardless of foam percentage. This is because the foam itself does not affect the matrix integrity and mechanical properties of the cementitious material. As expected, the strain at the peak UCS increased significantly (i.e., the specimen became much more ductile) when a thicker foam was used (see Table 3-1) – which is beneficial for the performance of pumpable roof supports. This is simply due to the large deformation of the foam itself even at a small load applied, as shown in Fig. A3-3.

	Before Test	During Test	After Test
(a)			
Foam → **(b)**			
(c)			

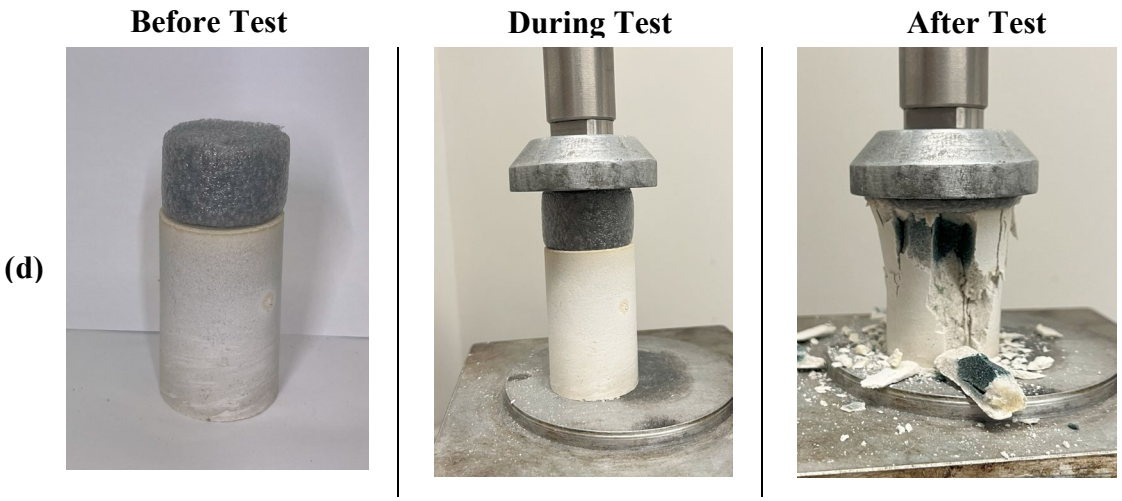
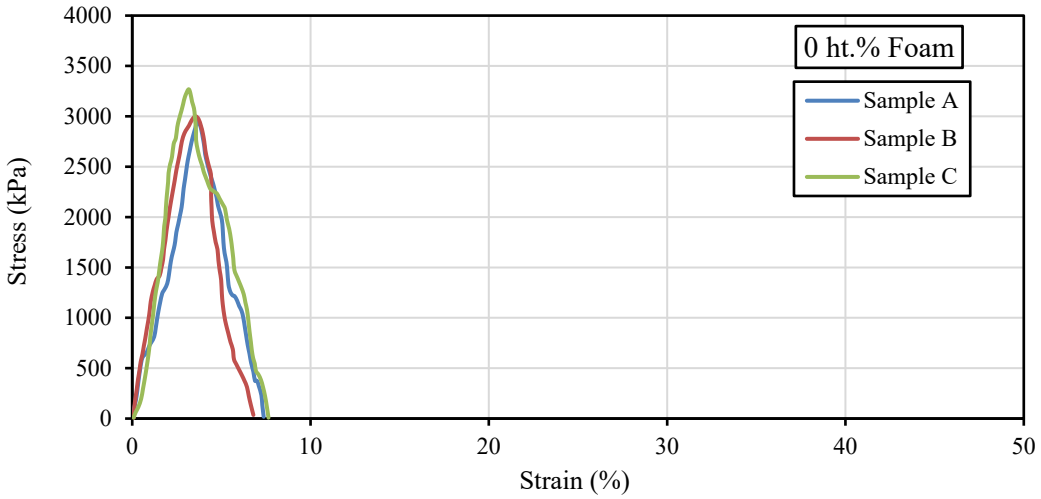
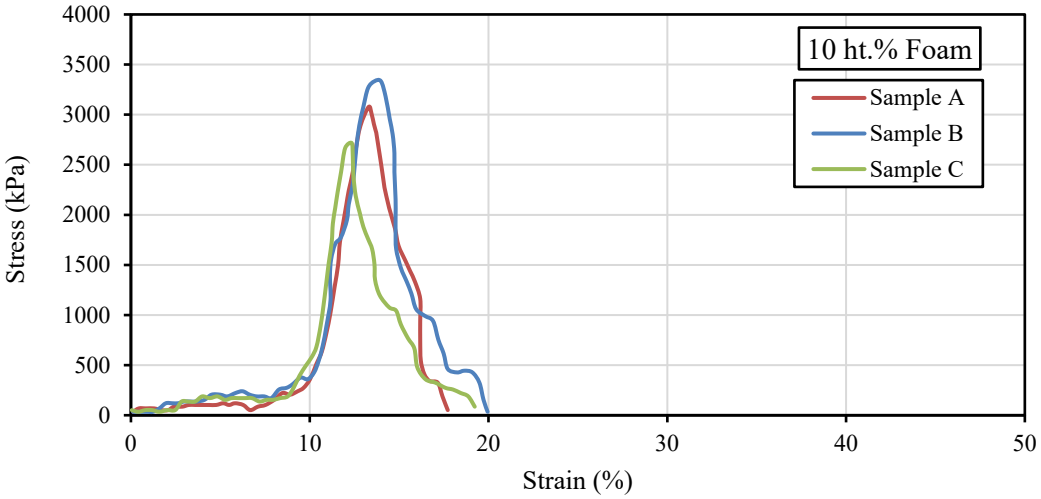
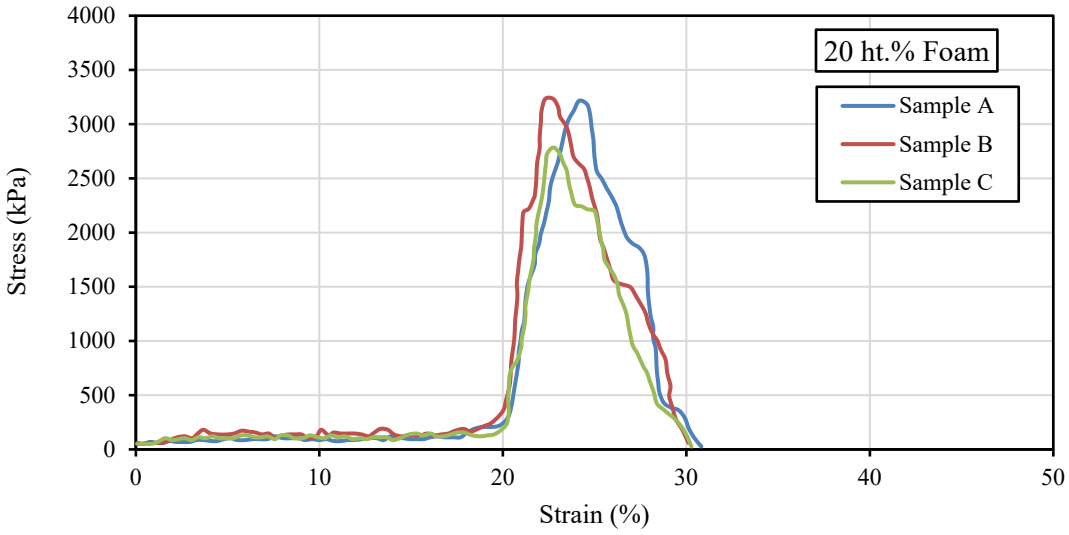


Fig. A3-1: Pictures of unbagged specimens prepared using foam as the top portion: (a) 0 ht.%, (b) 10 ht.%, (c) 20 ht.%, and (d) 30 ht.%.


0 ht.% Foam
Sample A
Sample B
Sample C
Stress (kPa)
Strain (%)
0
500
1000
1500
2000
2500
3000
3500
4000
0
10
20
30
40
50


10 ht.% Foam
Sample A
Sample B
Sample C
Stress (kPa)
Strain (%)
0
500
1000
1500
2000
2500
3000
3500
4000
0
10
20
30
40
50


20 ht.% Foam
Sample A
Sample B
Sample C
Stress (kPa)
Strain (%)
0
500
1000
1500
2000
2500
3000
3500
4000
0
10
20
30
40
50

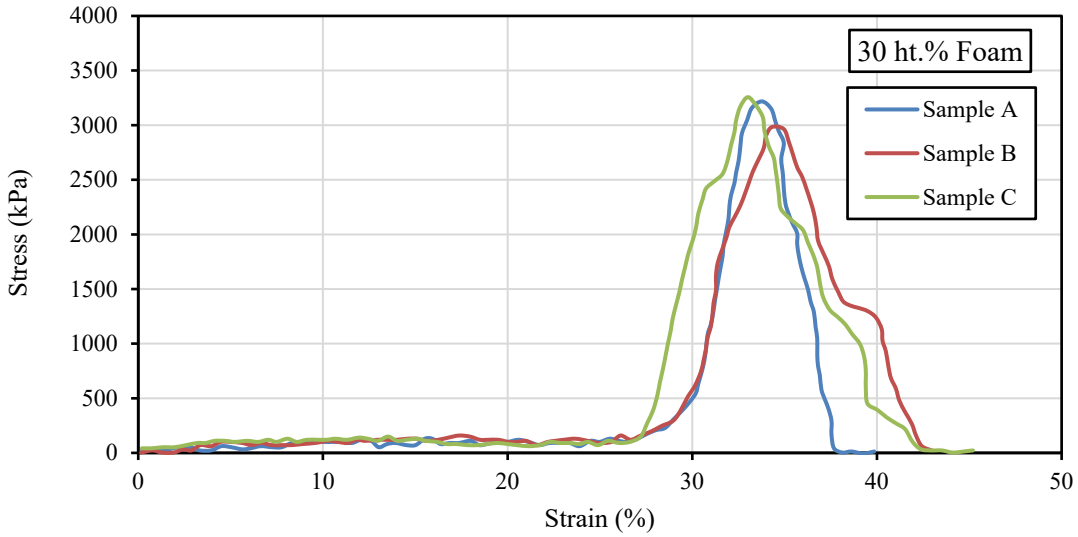


Fig. A3-2: Stress-strain curves of unbagged specimens prepared using foam as the top portion: (a) 0 ht.%, (b) 10 ht.%, (c) 20 ht.%, and (d) 30 ht.%.

Table A3-1: Summary of peak UCS and strain at peak UCS of unbagged specimens containing foam as the top portion.

Specimen	Peak UCS (MPa)	Strain at peak UCS (%)	Average peak UCS (MPa)	Average strain at peak UCS (%)
0 ht.% foam - A	2.94	3.64	3.07	3.45
0 ht.% foam - B	3.01	3.54		
0 ht.% foam - C	3.26	3.15		
10 ht.% foam - A	3.07	13.3	3.03	13.1
10 ht.% foam - B	3.33	13.6		
10 ht.% foam - C	2.71	12.3		
20 ht.% foam - A	3.21	24.2	3.06	23.0
20 ht.% foam - B	3.23	22.0		
20 ht.% foam - C	2.78	22.7		
30 ht.% foam - A	3.21	33.8	3.14	33.7
30 ht.% foam - B	2.98	34.3		
30 ht.% foam - C	3.25	33.0		

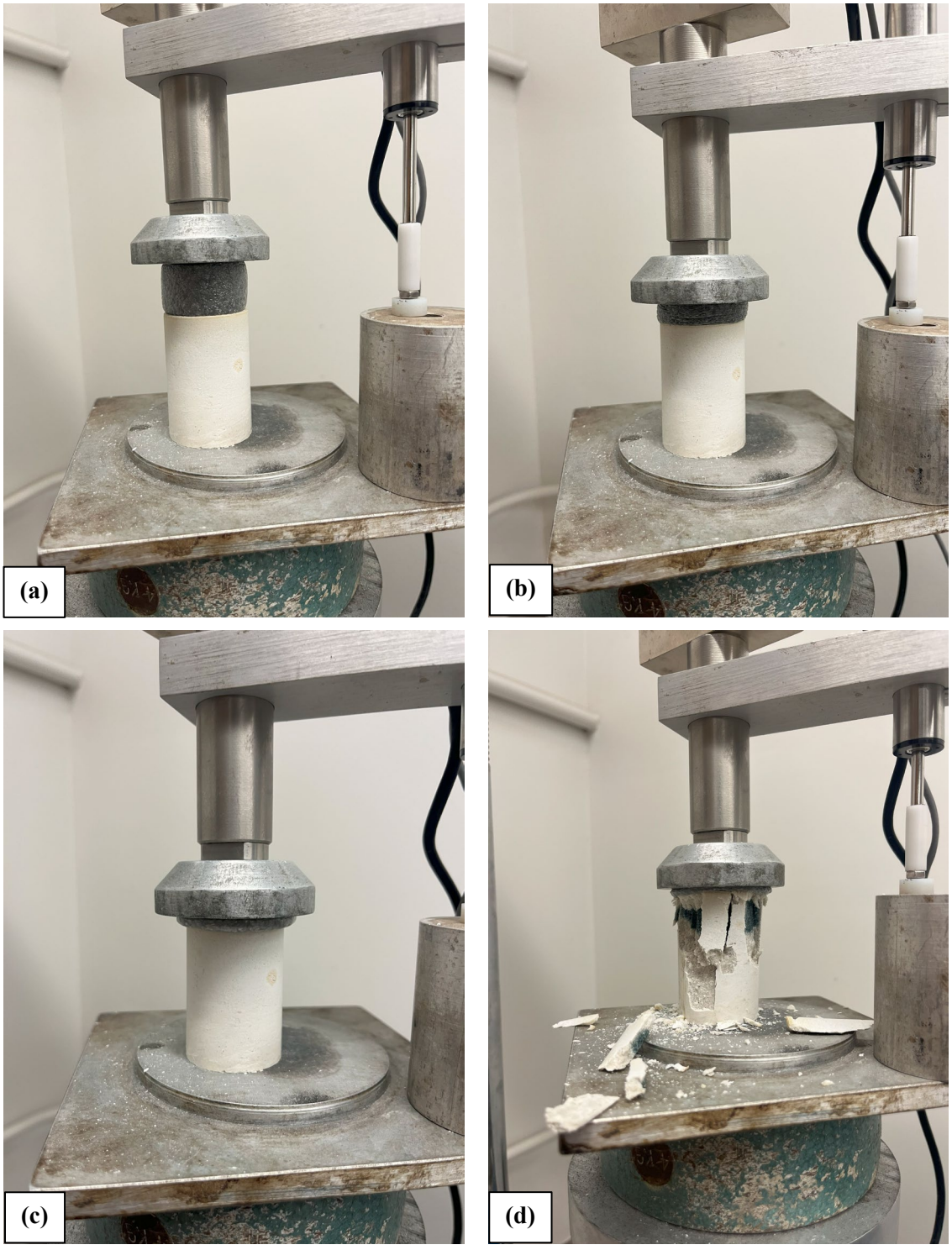


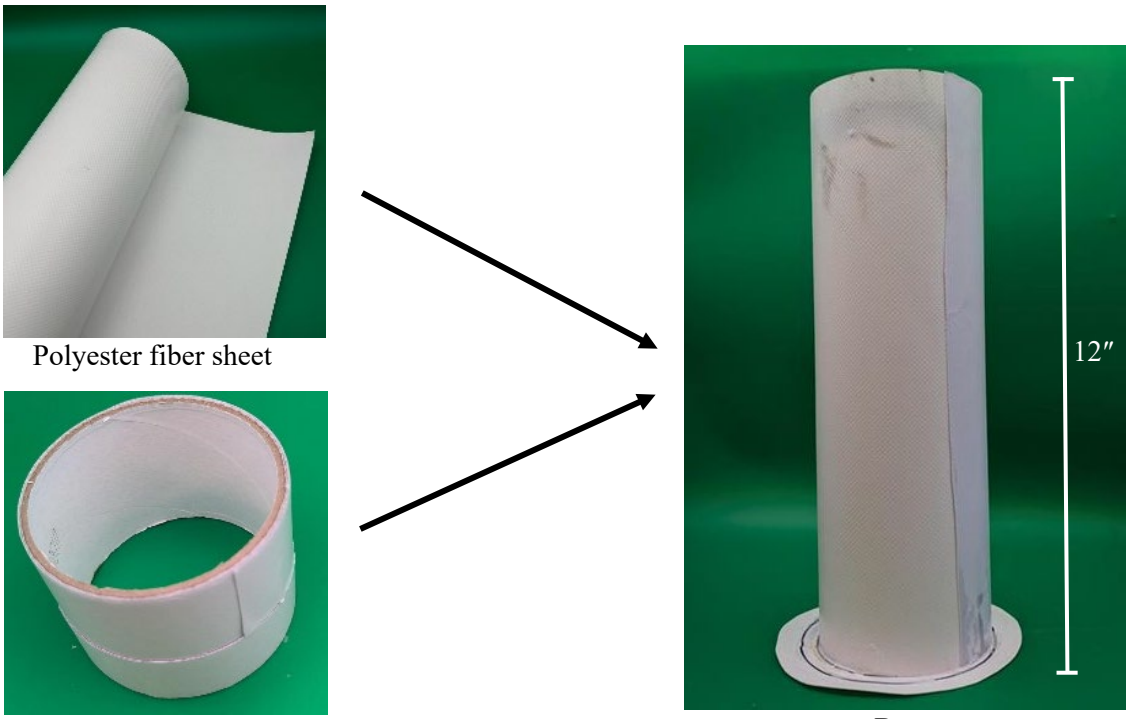
Fig. A3-3: Deformation of foam during the UCS test for specimens prepared with 30 ht.% of foam at strains of: (a) 0%, (b) 15%, (c) 30%, and (d) 34% (failure).

Appendix 4: Laboratory Experiments Using Internal Reinforcements

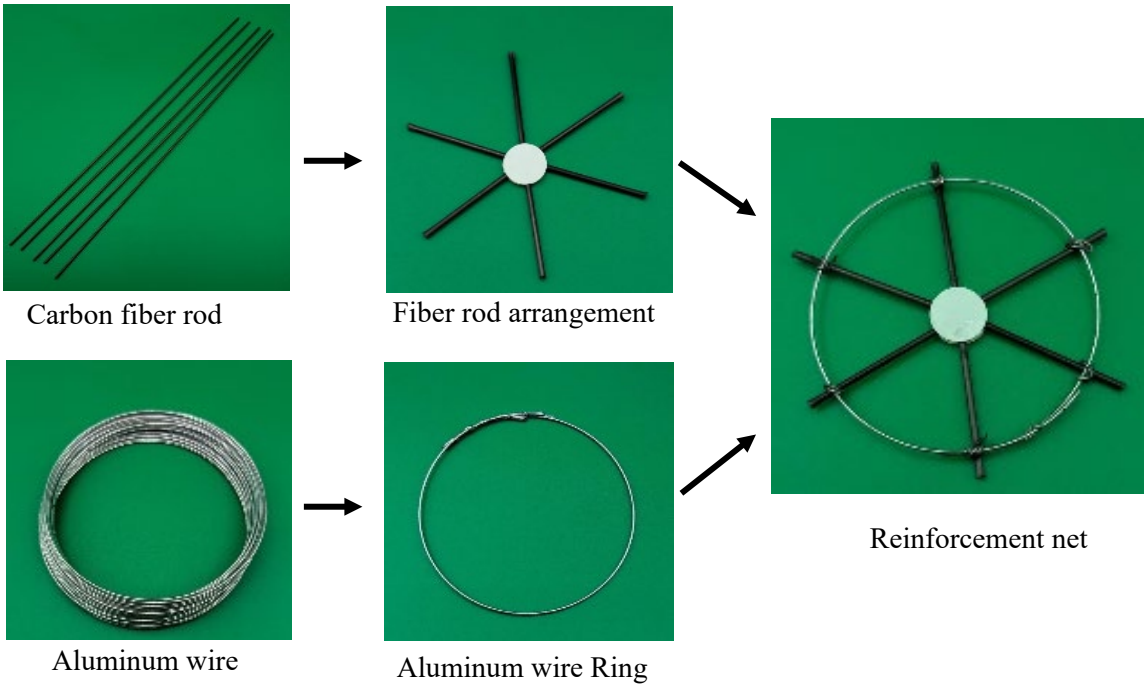
To address this limitation of using extremely light, highly compressible, micron-sized beads/spheres or highly deformable foam (see Appendix 2 and 3), we prepared bagged cylindrical specimens containing internal layers of reinforcing fibers to study the effect of internal reinforcements on the mechanical performance of the specimens. The following presents the results obtained.

A4.1 Preparation of Bagged Specimens Containing Internal Reinforcements

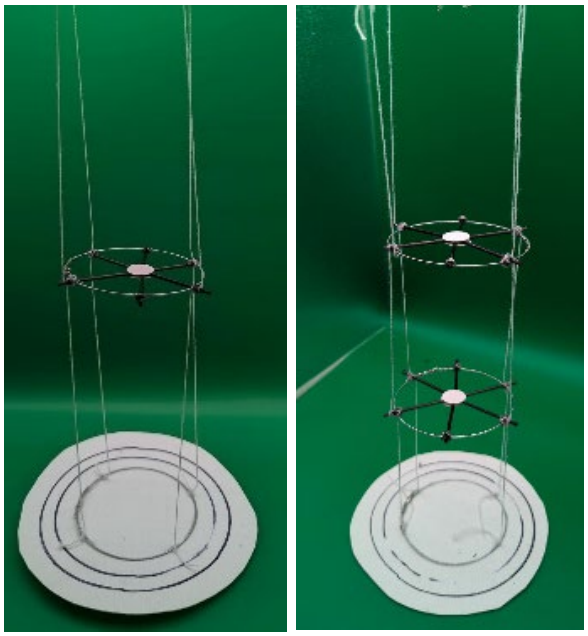
As a feasibility study, we selected a specimen size of 4 inches in diameter and 12 inches in length, yielding a length-to-diameter (L/D) ratio of 3. Fig. A4-1 illustrates the procedure for producing the bagged specimens containing internal reinforcements. In the first step (Fig. A4-1a), a polyester fiber sheet was cut into pieces measuring 12 inches in height and 13.6 inches in length. Each piece was rolled into a cylindrical shape with a height of 12 inches and a diameter of 4 inches (corresponding to a perimeter of 12.6 inches). Strong duct tape was applied along the overlapping edge, and sealant glue was used on the inner face of the overlap to create a robust bond. This ensured the bag maintained a circular shape and prevented grout leakage during casting. The base of each cylindrical bag was sealed with a circular piece of polyester fiber sheet. In the second step (Fig. A4-1b), the reinforcement nets were fabricated. Carbon fiber rods with a diameter of 2 mm were cut into equal lengths of 45 mm. Six of these rods were arranged with one end in contact and spaced at 60-degree intervals. The rods were bonded at the contact point using a high-strength adhesive. The assembly was further reinforced with a circular aluminum ring. In the third step (Fig. A4-1c), layers of reinforcement nets were connected at specified vertical spacings of 6, 4, or 3 inches using four flexible strings, corresponding to one, two, and three reinforcement layers (RL). These strings were anchored at the top and bottom of the bag to maintain the correct positioning of the reinforcement layers during grout pouring. In the final step (Fig. A4-1d), the two streams of the cementitious material were poured simultaneously into the bag to ensure homogeneity. Once the bag was filled, the top was sealed with a plastic film, and zip ties were installed circumferentially at equal intervals along the length of the bagged specimen. The specimens were cured at room temperature until the testing date. The specimen nomenclature and corresponding reinforcement arrangements are summarized in Table A4-1.



(a) Manufacturing Bag



(b) Manufacturing Fiber Reinforcing Net

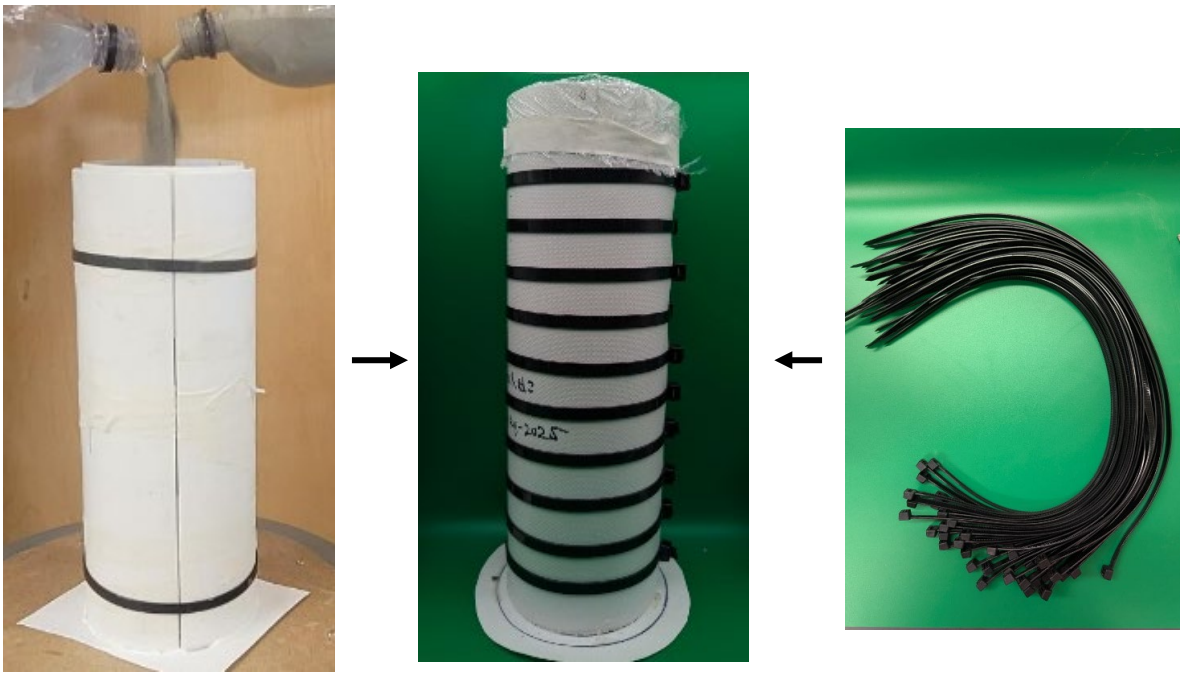


Arrangement of reinforcing net



View of reinforcements inside bag

(c) Arrangement of Reinforcements



Casting Mix

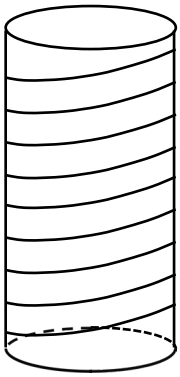
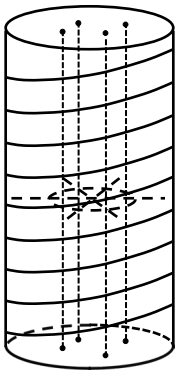
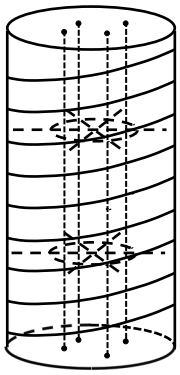
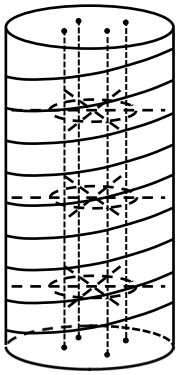
Curing stage

Zip Ties

(d) Casting and curing of specimens

Fig. A4-1: Procedure for producing bagged specimens with internal reinforcements.

Table A4-1: Illustration of reinforcement arrangements inside the confinement bag of PRS specimens with an internal bag diameter of 4 in.

No RL	One RL	Two RL	Three RL
			
No reinforcement	One layer of reinforcement at a vertical spacing of 6 in.	Two layers of reinforcement at a vertical spacing of 4 in.	Three layers of reinforcement at a vertical spacing of 3 in.

A4.2 Test Results and Discussion

A uniaxial compression test was performed on all the prepared bagged specimens. The stress-strain curves obtained were analyzed as shown in Fig. A4-2. The initial stiffness represents the linear portion of the stress-strain curve prior to peak stress, reflecting the specimen's resistance to deformation under the applied load. The sudden drops in load-bearing capacity following the peak stress are known as load-shed events. Following a load-shed event, the PRS may partially regain its load-bearing capacity which is called load restoration. The ability to sustain the bearing capacity over a wide strain range is referred to as its residual stress.

The stress-strain curves of the PRS specimens with No RL, One RL, Two RL, and Three RL are presented in Fig. A4-3. All PRS specimens exhibited a rapid increase in stress during the initial loading, indicating that the infill cementitious material developed its load-bearing resistance at relatively small strains, which is consistent with previously reported findings [1]. However, the peak stress and post-peak behavior were strongly influenced by the number of reinforcement layers. For the No RL specimens, the post-peak region exhibited several load-shed events accompanied by a continued decline in stress (Fig. A4-3a). This behavior is consistent with the failure mechanism of brittle cementitious materials in confined pumpable roof supports [2] where internal cracking of the cementitious material leads to abrupt load shedding. Consequently, the No RL specimens retained some load-bearing capacity beyond the peak stress, primarily due to the confinement from the containment bag and external ties, but the average stress declined progressively with increasing strain.

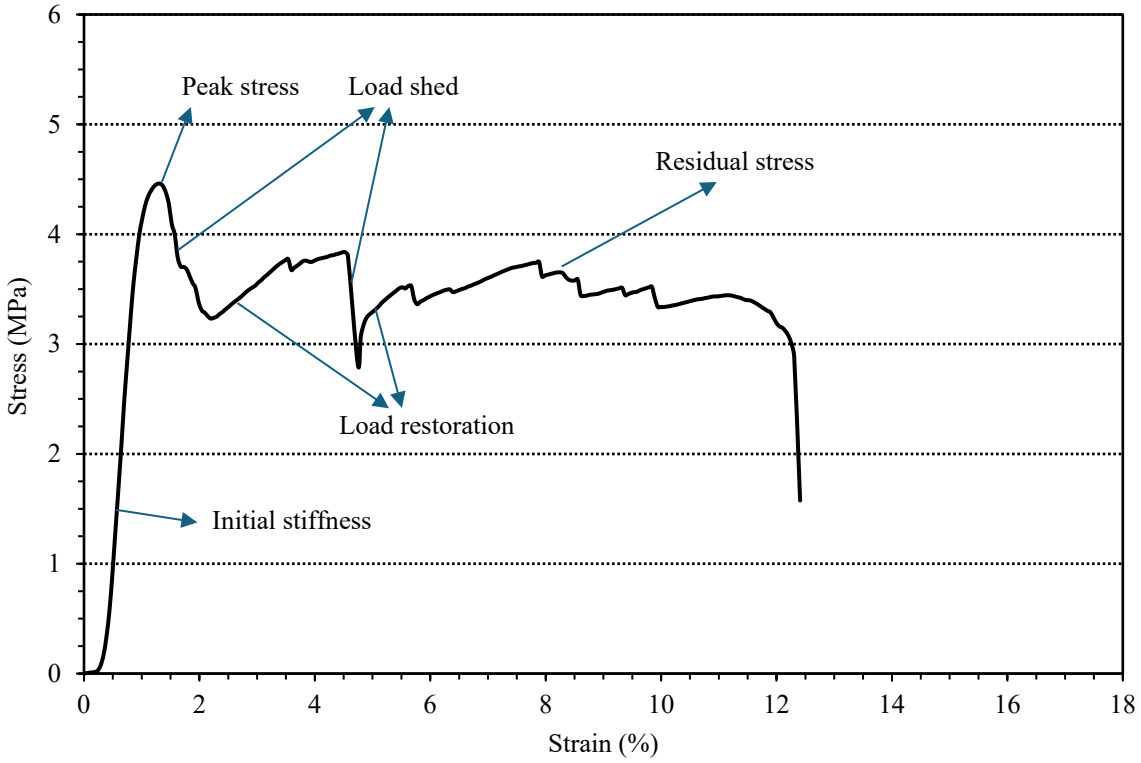
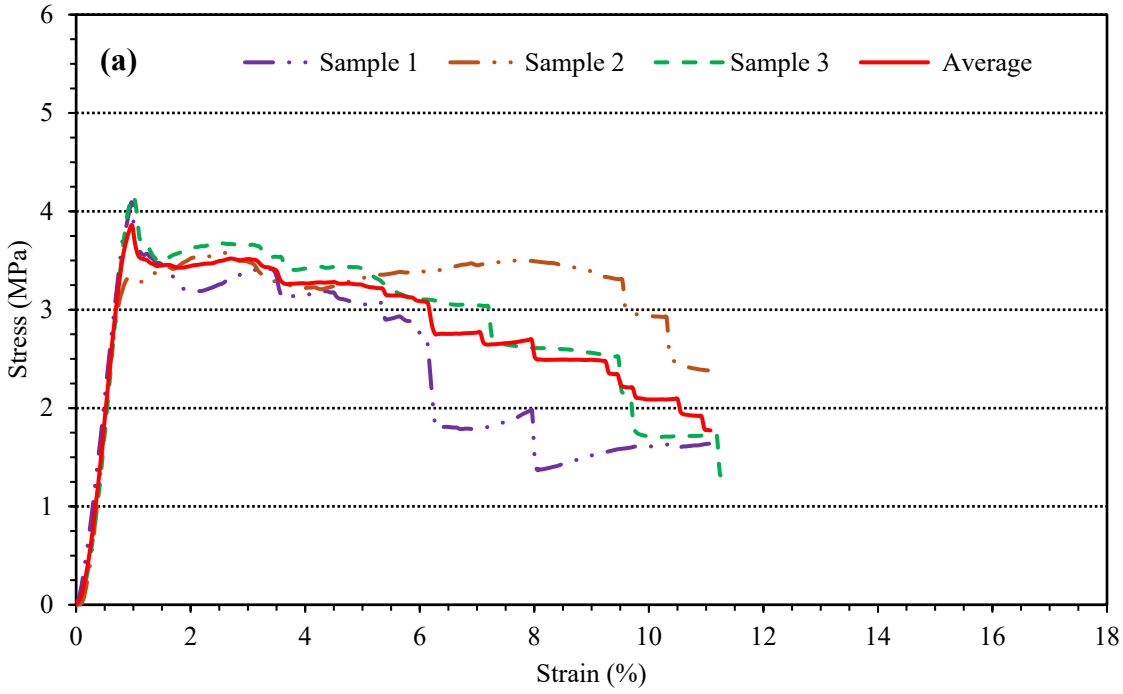
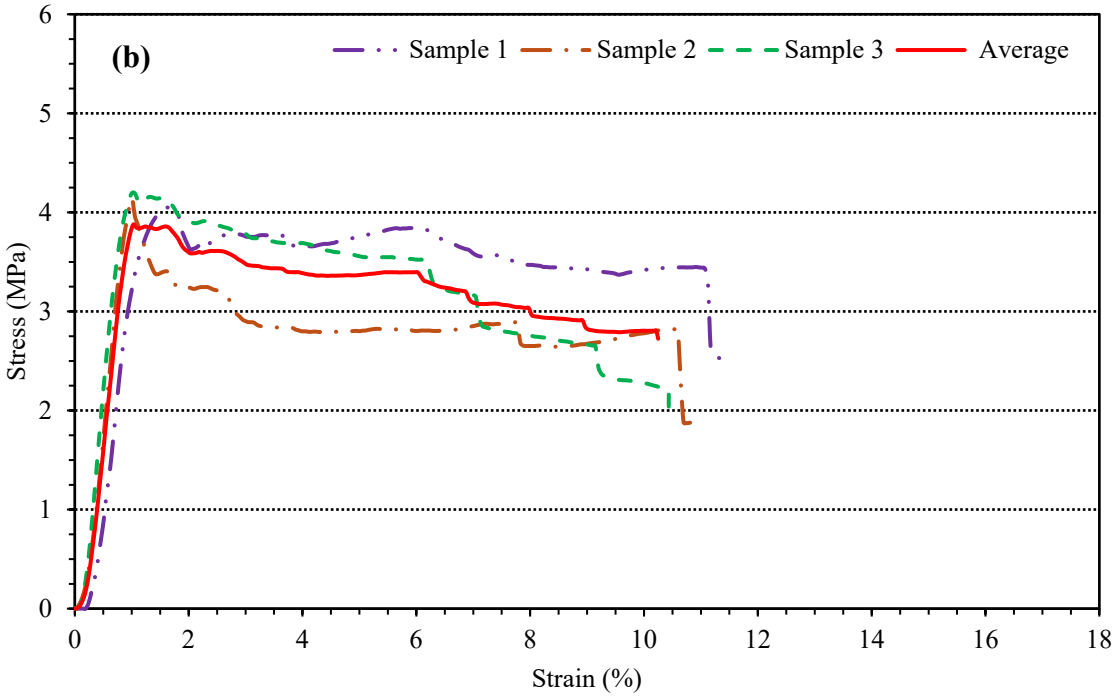


Fig. A4-2: Identification of performance characteristics of PRS from stress-strain curve.

The specimens containing reinforcement layers exhibited an increase in peak stress and a more stable post-peak response, with higher residual stress levels corresponding to the number of reinforcement layers. Compared with the No RL specimens, the Two RL and Three RL specimens demonstrated visible stress recovery following load-shed events (Figs. A4-3c and d) and retained higher residual stress throughout the residual loading region. This suggests that the internal reinforcement nets became engaged when the cementitious material cracked, thereby facilitating stress redistribution by maintaining confinement around the fractured material.


(a)
Sample 1
Sample 2
Sample 3
Average
Stress (MPa)
Strain (%)
0
1
2
3
4
5
6
0
2
4
6
8
10
12
14
16
18


(b)
Sample 1
Sample 2
Sample 3
Average
Stress (MPa)
Strain (%)
0
1
2
3
4
5
6
0
2
4
6
8
10
12
14
16
18

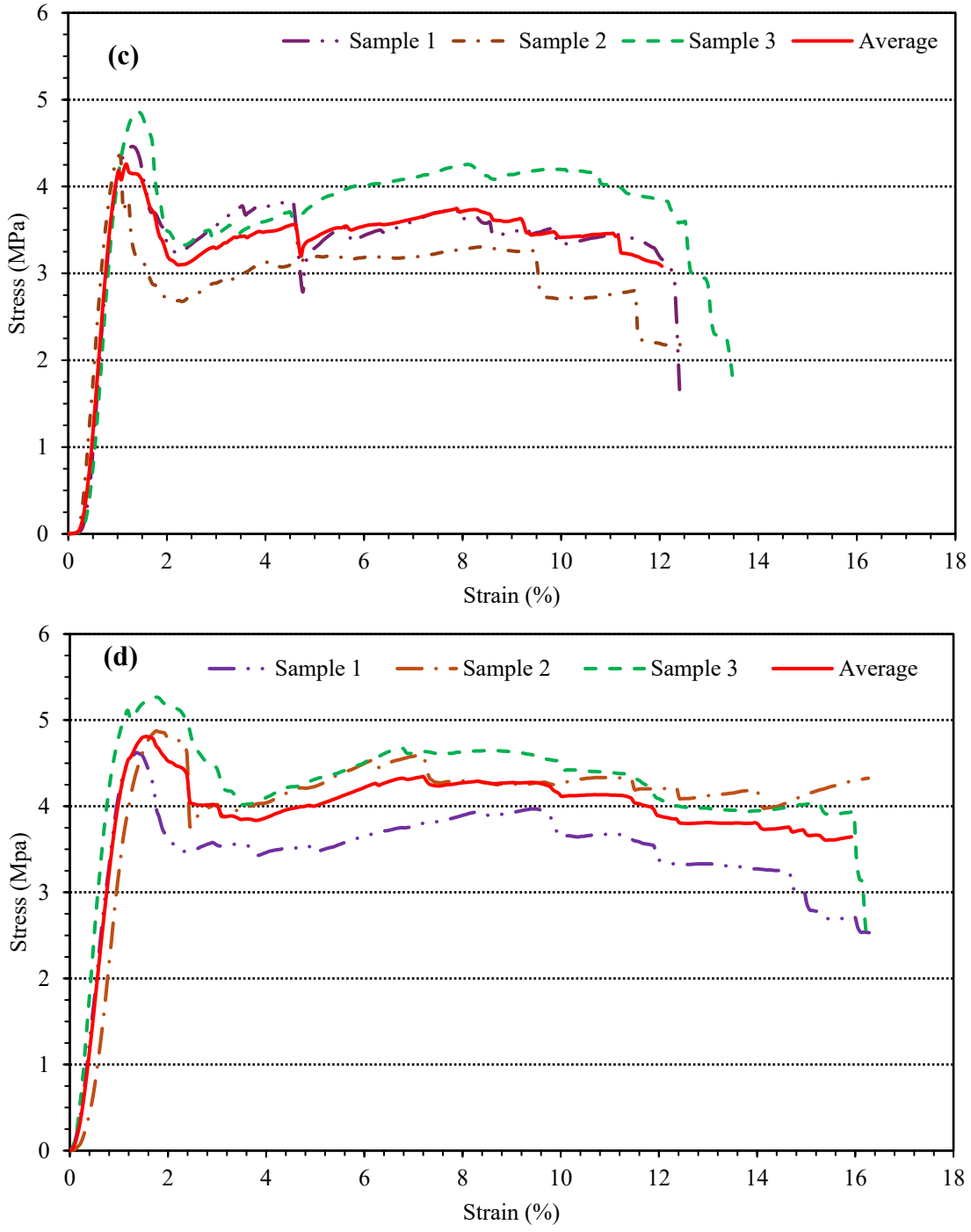


Fig. A4-3: Stress-strain curves of PRS specimens with: (a) no internal reinforcement; (b) one layer of internal reinforcement; (c) two layers of internal reinforcement; and (d) three layers of internal reinforcement.

The peak stress versus the strain at the peak stress of the PRS specimens with and without internal reinforcement layers is presented in Fig. A4-4. The peak stress increased progressively with a larger number of reinforcement layers. The No RL specimens reached an average peak stress of 3.85 MPa at 0.92% strain, while the One RL specimen reached a comparable peak stress of 3.87 MPa at 1.02% strain. This suggests that a single reinforcement layer was insufficient to significantly alter the peak stress, because the peak stress remained governed primarily by the infill cementitious matrix and the outer confinement bag and ties at a reinforcement spacing-to-diameter ratio of 1.5 [3]. The Two RL specimens reached an average peak stress of 4.25 MPa at 1.17% strain, representing an increase of approximately 10.4% relative to the No RL specimens. The Three RL specimens achieved the highest average peak stress of 4.80 MPa at 1.52% strain, corresponding to an improvement of approximately 24.7% over the No RL specimens. Furthermore, the strain at peak stress increased significantly, by approximately 10.9%, 27.2%, and 65.2% for the One RL, Two RL, and Three RL specimens, respectively, compared with the No RL specimens. Therefore, the reinforcement not only increased the peak stress but also delayed the onset of failure, allowing the support to deform more before reaching its maximum capacity.

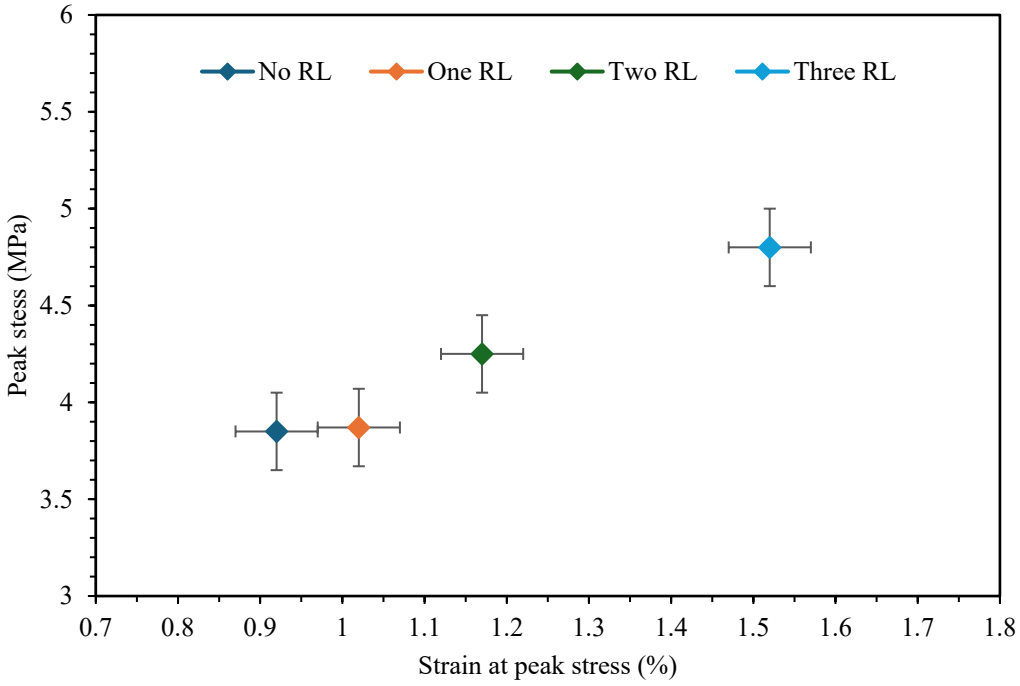


Fig. A4-4: Peak stress versus strain at peak stress of non-reinforced and reinforced PRS specimens.

The improvement in peak stress can be attributed to the additional confinement provided by the internal reinforcement nets. Mander et al. [4] demonstrated that transverse reinforcement enhances the strength and ductility of axially loaded cementitious members by generating effective lateral confining stresses. The effectiveness of this confinement depends on the arrangement and spacing of the transverse reinforcement, as arching action develops between adjacent reinforcement layers

[4]. In the No RL specimens, the lateral dilation of the infill cementitious core was resisted primarily by the containment bag and external ties. In the reinforced specimens, the internal reinforcement nets provided additional lateral restraint. Increasing the number of reinforcement layers and reducing the spacing between them decreased the extent of weakly confined regions, enhanced the effective confinement of the infill cementitious core, and delayed the development of unstable crack propagation.

The failure patterns observed after the uniaxial compression tests (Fig. A4-5) further support this interpretation. The No RL specimen (Fig. A4-5a) exhibited extensive splitting, lateral separation, and loss of structural integrity, corresponding to a Type II failure as defined by ASTM C39, due to the absence of internal reinforcement. The two RL and three RL specimens (Figs. A4-5b and c) exhibited a distinct diagonal fracture, corresponding to a Type IV failure under ASTM C39, and the location of the diagonal failure surface differed between the two types of specimens due to the constraints from the internal reinforcements. Although localized fractures remained visible, the three RL specimens (Fig. A4-5d) exhibited overall integrity, suggesting that the internal reinforcements restrained lateral dilation and retained the fractured infill cementitious core within the bag. This explains why the three RL specimens exhibited the highest peak stress and the largest strain at peak stress.

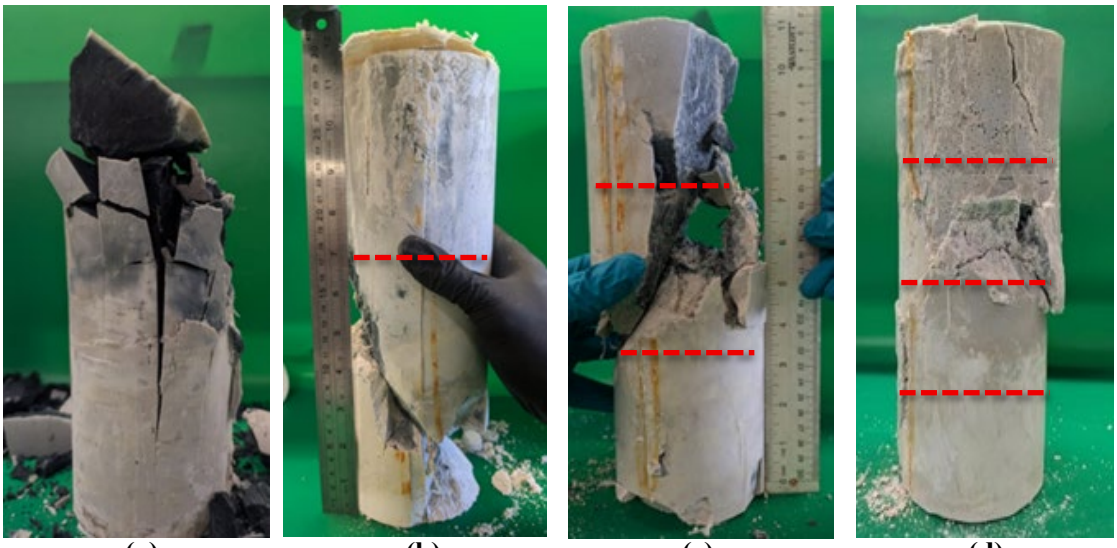


Fig. A4-5: Failure modes of PRS specimens containing: (a) no internal reinforcement; (b) one layer of internal reinforcement; (c) two layers of internal reinforcement; and (d) three layers of internal reinforcement. The red dashed lines indicate the location of internal reinforcement layers.

A sudden drop in load, referred to as a load-shed event, provides important information about the post-peak stability of PRSs [5]. Fig. A4-6 presents the number of load-shed events recorded for all four types of specimens before 8% strain. The No RL specimens exhibited five load-shed events, while the One RL, Two RL, and Three RL specimens exhibited four, two, and one load-shed event, respectively. The progressive reduction in load-shed events indicates that the internal reinforcement layers reduced the frequency of unstable fracture initiation and propagation within the cementitious infill core and improved the post-peak stability of the PRS. Load-shed events are associated with the brittle fracture of the cementitious infill core and a corresponding degradation of the load-bearing response [5]. Therefore, the lower number of load-shed events observed in the reinforced specimens suggests that the internal reinforcement nets limited the progressive deterioration of the fractured infill core and facilitated a more stable post-peak response.

The load (stress) restoration events further support this interpretation. The No RL and One RL specimens did not exhibit clear restoration events, indicating that load-shedding continued after peak stress and the specimens were unable to regain their load-bearing capacity (Figs. A4-3a and b). In contrast, the Two RL and Three RL specimens exhibited stress restoration following load-shed events, maintaining a more stable and continuous stress response. Upon cracking of the cementitious infill core, the internal reinforcement nets restrained lateral dilation and preserved the integrity of the fractured infill core, allowing the Two RL and Three RL specimens to partially regain their load-bearing capacity after certain load-shed events. These findings are consistent with previous studies on FRP-confined cementitious grout for standing supports, which reported that improved confinement promotes strain-hardening behavior, enhances axial deformation capacity, and maintains structural integrity after damage initiation in the cementitious grout [2,3].

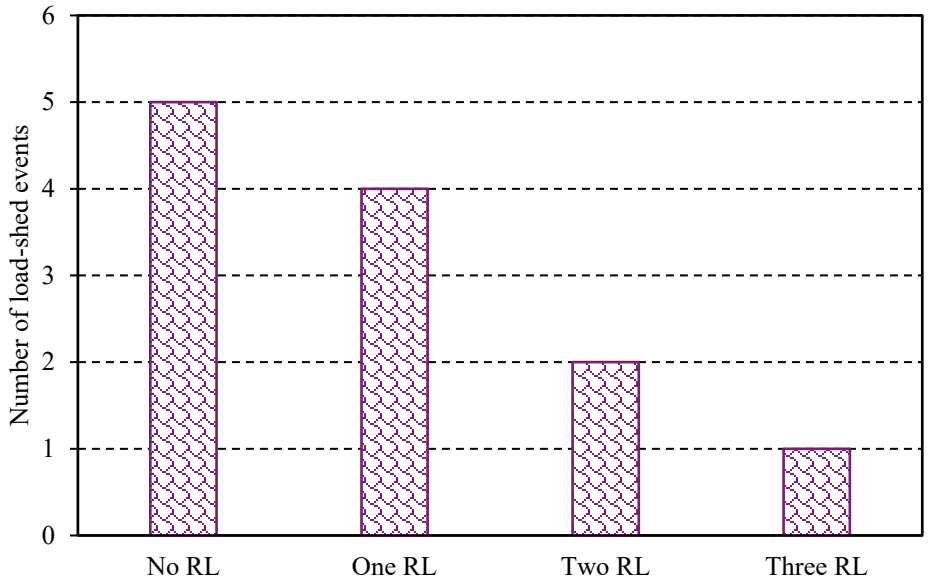


Fig. A4-6: Number of load-shed events for non-reinforced and reinforced PRS specimens before 8% strain.

The average residual stress at 8% strain for all four types of specimens is presented in Fig. A4-7, showing a consistent increase with a higher number of reinforcement layers. Specifically, the average residual stress was 2.96 MPa, 3.71 MPa, and 4.27 MPa for the One RL, Two RL, and Three RL specimens, respectively, representing an increase of 17.9%, 47.8%, and 70.1% over the 2.51 MPa for the No RL specimens. The residual stress improvement represents one of the most significant outcomes of the proposed internal reinforcement concept, as PRSs must continue to carry load after the cementitious infill core has cracked and entered the post-peak region. Batchler [5] reported that the residual load capacity of a PRS is strongly dependent on the integrity of confinement after infill fracture. The fractured cementitious infill core continues to dilate and bulk under increasing convergence, while the surrounding confinement system restrains the material and allows the support to sustain a useful residual load [5].

Under the same confinement system, the enhanced residual stress observed in the reinforced specimens can be attributed to the ability of the internal reinforcement nets to retain and confine the cracked cementitious infill core. After the peak stress, the matrix no longer behaves as an intact continuum; instead, the fractured material tends to dilate, rearrange, and exert lateral pressure on the surrounding confinement system. A similar mechanism has been reported for FRP-confined cementitious infill materials. Li et al. [2] observed that lateral expansion increased after fracture of the infill core, activating the CFRP confinement and improving the post-cracking bearing response [2]. Harries and Kharel [6] similarly demonstrated that passive confinement is mobilized by lateral dilation of a cementitious core and that greater confinement improves the axial stress-strain response [6]. In the present study, the internal reinforcement nets provided additional localized restraint at multiple elevations along the specimen height, maintaining the fractured cementitious infill core in a consolidated state within the containment bag. This decreases the dependence of the post-peak response on the bag alone and allows the reinforced specimens to sustain a higher residual stress at large strains, demonstrating that the proposed reinforcement concept effectively preserved the residual load-bearing capacity of PRSs under large deformation conditions.

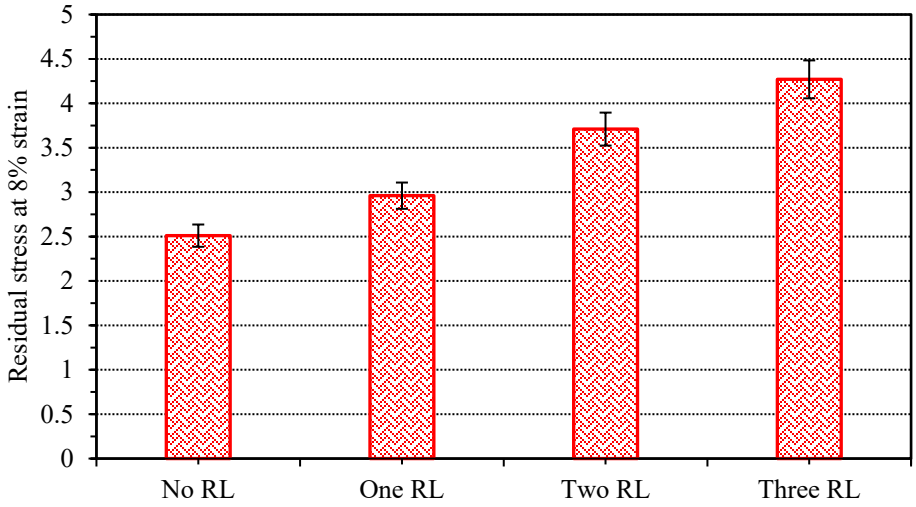


Fig. A4-7: Residual stress of non-reinforced and reinforced PRS specimens at 8% strain.

Fig. A4-8 shows the average stress-strain response for the unreinforced and reinforced PRS specimens, clearly demonstrating the improvement in the performance characteristics described earlier with increasing number of internal reinforcement layers. Again, the improvement can be attributed to a confinement-restoration mechanism. During axial loading, the cementitious infill matrix initially resists the applied stress as a solid column. In the No RL specimens, as strain increased, internal cracking initiated and a well-formed cone developed at one end, followed by vertical cracks propagating axially through the specimen (Fig. A4-5a). This failure mode corresponds to Type II failure as defined by ASTM C39. In the No RL specimens, lateral dilation was resisted primarily by the outer bag and ties, and once the fractured material compromised the integrity of the confinement bag and ties, the support underwent load shedding and exhibited reduced residual bearing capacity [7].

In the reinforced specimens, the failure mode transitioned to a diagonal fracture, classified as Type IV failure under ASTM C39. Notably, the location of the diagonal failure surface differed among the One RL, Two RL, and Three RL specimens, as shown in Figs. A4-5b, c, and d, confirming that the internal reinforcement altered both the failure mode and failure location. In the reinforced specimens, the internal reinforcement nets acted as localized restraints that interrupted lateral expansion and limited crack opening, improving the stress state of the cementitious infill core by maintaining confinement after cracking.

The number of load-shed events decreased progressively from five in the No RL specimens to only one in the Three RL specimens (Fig. A4-6), indicating a transition from brittle load loss toward a much more ductile and stable post-peak response. For field PRS applications, this behavior is particularly desirable, as a support that maintains residual bearing capacity after cracking can continue to resist roof-to-floor convergence and provide a safer load-bearing system under large deformation conditions [8]. Consequently, the internal reinforcement layers acted as effective restraints within the PRS, limiting crack propagation and preserving confinement after matrix failure.

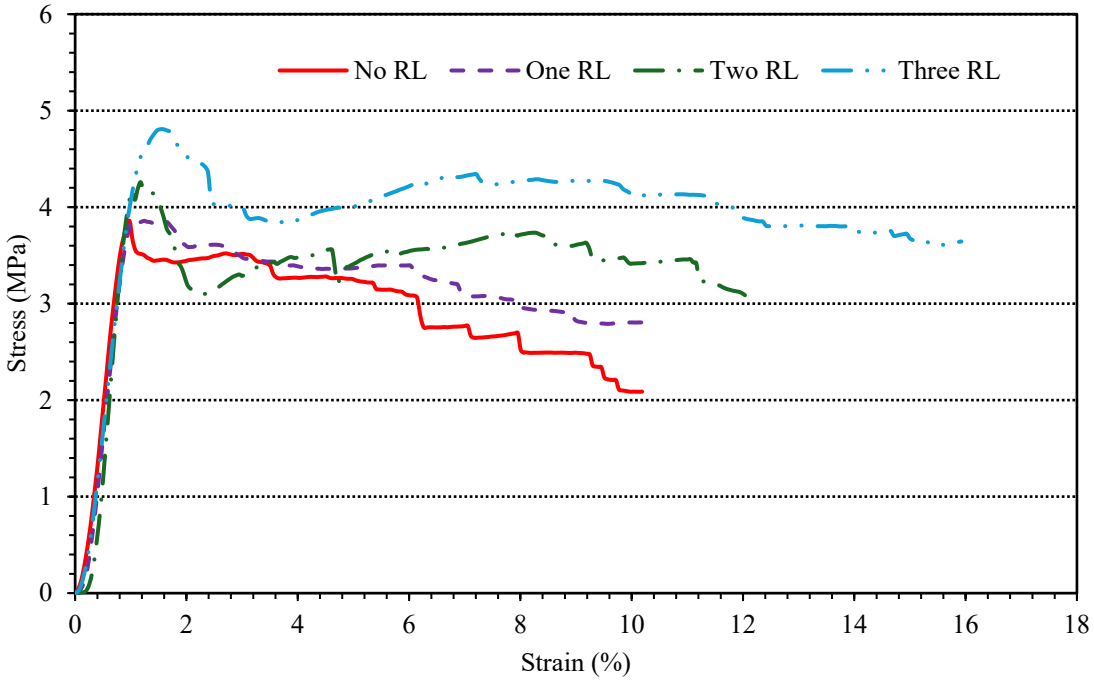


Fig. A4-8: Average stress-strain behavior for non-reinforced and reinforced PRS specimens.

A4.3 References

[1] A. Nikvar-Hassani, L. Zhang, Development of a biopolymer modified geopolymer based cementitious material for enhancement of pumpable roof support, Mater. Struct. 55 (2022) 116.

[2] G. Li, H. Liu, W. Deng, H. Wang, H. Yan, Behavior of CFRP-confined sand-based material columns under axial compression, Polymers (Basel). 13 (2021) 3994.

[3] H. Zhao, T. Ren, A. Remennikov, A hybrid tubular standing support for underground mines: Compressive behaviour, Int. J. Min. Sci. Technol. 31 (2021) 215–224.

[4] J.B. Mander, M.J.N. Priestley, R. Park, Theoretical stress-strain model for confined concrete, J. Struct. Eng. 114 (1988) 1804–1826.

[5] T. Batchler, Analysis of the design and performance characteristics of pumpable roof supports, Int. J. Min. Sci. Technol. 27 (2017) 91–99.

[6] K.A. Harries, G. Kharel, Experimental investigation of the behavior of variably confined concrete, Cem. Concr. Res. 33 (2003) 873–880.

[7] D. Zhang, J. Bai, Z. Zhang, Q. Zhu, M. Deng, S. Yan, R. Wang, S. Liu, Field and Numerical Investigations on Pumpable Standing Supports Failure Analysis in the Longwall Pre-driven Recovery Room, Rock Mech. Rock Eng. 58 (2025) 1199–1220.

[8] T.M. Barczak, S.C. Tadolini, Pumpable roof supports: an evolution in longwall roof support technology, (2008).

9.0 Acknowledgement/Disclaimer

This study was sponsored by the Alpha Foundation for the Improvement of Mine Safety and Health, Inc. (ALPHA FOUNDATION). The views, opinions and recommendations expressed herein are solely those of the authors and do not imply any endorsement by the ALPHA FOUNDATION, its Directors and staff.